

Emergent U(1) gauge theory with fractionalized boson/fermion from the bose condensation of exciton in multi-band insulator

Sung-Sik Lee and Patrick A. Lee

*Department of Physics, Massachusetts Institute of Technology,
Cambridge, Massachusetts 02139, U.S.A.*

(Dated: January 26, 2020)

Fractionalized phases are studied in a low energy theory of exciton bose condensate in a multi-band insulator. It is shown that U(1) gauge theory with either fractionalized boson or fermion can emerge out of a single model depending on the coupling constants. Both the statistics and spin of the fractionalized particles are dynamically determined, satisfying the spin-statistics theorem in the continuum limit. We present two mutually consistent descriptions for the fractionalization. In the first approach, it is shown that fractionalized degree of freedom emerges from reduced phase space constrained by strong interaction and that the U(1) gauge field arises as a collective excitation of the low energy modes. In the second approach, complimentary descriptions are provided for the fractionalization based on world line picture of the original excitons. The emergent gauge structure is identified from the fluctuating web of exciton world lines which, in turn, realizes the string net condensation in a space-time picture.

I. INTRODUCTION

Fractionalization is a phenomenon where a microscopic degree of freedom in many-body system decays into multiple modes by strong interaction. For example, it is well known that interacting electrons in 1+1D decay into spin and charge density waves[1]. In 2+1D, electrons under strong magnetic field decay into quasiparticles carrying only fraction of the electron charge[2]. Given the novelty of the phenomena, it is natural to ask whether the fractionalization can occur more ubiquitously in other systems.

Possible fractionalized phases have been extensively studied in 2+1D quantum spin system in view of its relevance to high temperature superconductivity (a comprehensive review for this approach can be found in Ref.[3]). Earlier, Anderson proposed that a neutral spin-1/2 excitation, dubbed as spinon, can arise in a quantum disordered (spin liquid) phase of 2+1D antiferromagnet[4]. In gauge theory picture various mean-field states have been found which have the spinon excitation along with a Z_2 gauge field[5, 6, 7, 8]. Since the Z_2 gauge field is discrete, the deconfinement phase can be stable with massive or massless spinon excitations. If gauge group is continuous like U(1), the deconfinement phase with massive spinon is not stable at zero temperature in 2+1D owing to the proliferation of instantons[9]. At zero temperature, the deconfinement phase can occur if there is a time-reversal symmetry breaking[10], or there are massless modes[11, 12, 13] protected by lattice symmetry[8].

The existences of the deconfinement phase have been also demonstrated in an exact soluble spin model[14, 15] and a dimer model in frustrated lattice[16]. More recently, various 3+1D models have been constructed which show deconfinement phases[17, 18]. These models have played an important role in studying the existence of the fractionalized phase. However they usually involve spin degrees of freedom defined on bond centers of lattices

or four spin interaction which break the rotation symmetry in spin space. At the same time bosonic models have been constructed which may be realized in principle in Josephson junction arrays[19, 20]. It is clearly of interest to search for more examples of realistic models which support fractionalization.

In a sense the fractionalization is opposite to the phenomena where multiple particles are bound to form a composite particle at low energy, such as molecules made of atoms and proton (neutron) made of quarks. The latter phenomena look more natural in the sense that larger structure is constructed from smaller building blocks. Fractionalization seems to work in the opposite direction. The puzzling nature of it becomes sharper when we realize that the fractionalization is about low energy physics. Fractionalization concerns the emergence of atom-like objects out of ‘molecules’ at low energy, not probing real ‘atoms’ inside ‘molecules’ at high energy. This conceptual difficulty of identifying fractionalized degree of freedoms out of original particle translates into the difficulty in the formalism to find a unique way of decomposition. There is no unique way of assigning statistics and spin to fractionalized particles. For example, spin liquid phase can be described either by bosonic spinon[5] or fermionic spinon[6]. Why should we choose one way of decomposition over another? More importantly, what is the fractionalized particle (emergent atom) after all, if it is not the real constituent (real atom) inside the original particle (molecules)?

The purpose of the present paper is to answer these questions by demonstrating that not only the emergence of fractionalized particle but also the statistics and spin of the fractionalized particle are all consequences of the intrinsic dynamics of the model. We explicitly show that both fractionalized boson and fermion can emerge out of a single theory depending on coupling constants, and that the spin and charge of the fractionalized particles are also uniquely determined from dynamical constraint.

The microscopic system we consider is a model describing excitons in multi-band insulator.

Since fractionalization is a rather unfamiliar concept in condensed matter physics, the question is often asked, how is it possible to visualize the new particles and the gauge field in terms of the original particle? In this paper we provide an answer by constructing a world line representation of the fractionalized particles and the gauge field in terms of the world lines of the original particles, which are in our case excitons. The world line (or duality) picture is complimentary to the more common field theoretical derivation, in that the confined state which is difficult to treat in field theory language, is easier to visualize. Furthermore, a qualitative understanding of the transition between confined and deconfined phases is possible in terms of pictures. It is our hope that by explicitly working out this example using both methods, we can gain deeper insights into these fascinating new phenomena.

We consider a system of spinless fermions with N degenerate bands where each band is composed of a conduction band and a valence band. The Hamiltonian is

$$\begin{aligned}
H = & \sum_{a=1}^N \sum_k \left[(\epsilon_k^c - \mu) c_k^{a\dagger} c_k^a + (\epsilon_k^d - \mu) d_k^{a\dagger} d_k^a \right] \\
& + U \sum_{a=1}^N \sum_k (c_k^{a\dagger} d_k^a + d_k^{a\dagger} c_k^a) \\
& - \frac{1}{v} \sum_{a,b} \sum_{k,k',q} V_q^{ab} c_{k+q}^{a\dagger} c_k^a d_{k'+q}^b d_{k'}^{b\dagger}. \quad (1)
\end{aligned}$$

Here c_k^a (d_k^a) is the annihilation operator of the fermion in the a -th conduction (valence) band, ϵ_k^c (ϵ_k^d), the energy dispersion of the conduction (valence) band. μ is the chemical potential. For simplicity we set $\epsilon_k^c - \mu = \Delta^c + \frac{k^2}{2m^c}$ and $\epsilon_k^d - \mu = -\Delta^d - \frac{k^2}{2m^d}$. The band gap is $\Delta^c + \Delta^d$ and μ is tuned so that there is equal density of conduction particle and valence hole. The index a labels the band degeneracy which is N for both conduction and valence bands. We imagine that the index labels orbital degeneracy, but we shall refer to it as the flavor index following the particle physics literature. U is the overlap integral which admixes the conduction and valence bands. V_q^{ab} is the strength of the Coulomb repulsion between fermions in band a and band b . It is assumed that the Coulomb interaction is local in real space and that the strength of the interaction depends on whether fermions are in a same band or in different bands, that is, $V_q^{ab} = V + V' \delta_{ab}$. $v = L^{D-1}$ is the volume of the system in d space dimension $d = (D - 1)$. We single out the attractive interaction between conduction particle and valence hole. The rest of the Coulomb interaction is assumed to be already included in the band structure determination of $\Delta^c + \Delta^d$ by the Hartree-Fock approximation.

The attractive interaction leads to a bound state between particle and hole which is an exciton. If the inter-

action energy is smaller than band gap, the exciton state lies between the gap. Since it is metastable, the fermion and hole will eventually recombine in a finite time. If the binding energy is large enough to overcome the band gap, particles and holes are spontaneously created to form a Bose condensate in the ground state. We will consider the latter case.

To fix ideas, it is useful to consider one particular realization of this model. Consider a hetero-junction where two thin semiconductor layers are separated by a thin barrier, shown schematically in Fig. 1. The energy $\Delta^c + \Delta^d$ is the separation between the bottom of the conduction on the left hand side and the top of the valence band on the right, and can in principle be tuned by applying a voltage. U is the tunneling matrix element of an electron across the barrier. In our model only electrons in bands with the same orbital index are allowed to tunnel, which is reasonable if we assume that different orbitals are orthogonal to each other due to their symmetry within the plane. If the Coulomb attraction between an electron on the left and a hole on the right is strong, a finite density of excitons will form spontaneously in the ground state, resulting in a Bose condensate of excitons. In real experiments it has proven difficult to realize the Bose condensation of excitons in the bulk, because the excitons tend to have attractive interaction, leading to the formation of exciton molecules or electron-hole liquid ground states. The most promising current example is indeed the layer geometry shown in Fig. 1 in GaAs hetero-junctions. Instead of using a bias voltage, the conduction and valence bands are populated by optical pumping, leading to a meta-stable state[21]. The dipolar interaction between the excitons assures that they are repulsive, making the system a promising candidate for exciton condensation. Here we are mostly interested in Eq. (1) as a model system which we assume can be realized in both two and three dimensions. The presence of N degenerate bands lead to additional complication in that there can be N^2 species of excitons and some or all of them may or may not condense. The order parameter for exciton condensation is

$$\bar{\chi}^{ab} = \langle d_i^{b\dagger} c_i^a \rangle, \quad (2)$$

where i is a site index. In this paper we examine the case where $\bar{\chi}^{aa} = \chi_d \neq 0$, i.e., the diagonal exciton are condensed. While it is possible that the symmetry breaking happens spontaneously, the presence of the U term in Eq. (1) explicitly breaks the symmetry and assures that $\bar{\chi}^{aa} \neq 0$. (In the case where the condensation of diagonal excitons occurs spontaneously, we can set $U = 0$ in our model.) We also assume that there is a finite amplitude for off diagonal exciton condensation. In appendix A we work out the mean field theory to show that this assumption is locally stable in some parameter range. In the remainder of the paper we examine the effect of phase fluctuations of $\chi^{ab} = \chi_o e^{i\theta^{ab}}$, to see whether the off-diagonal condensate may be destroyed, and to see under what circumstances a novel state of matter with

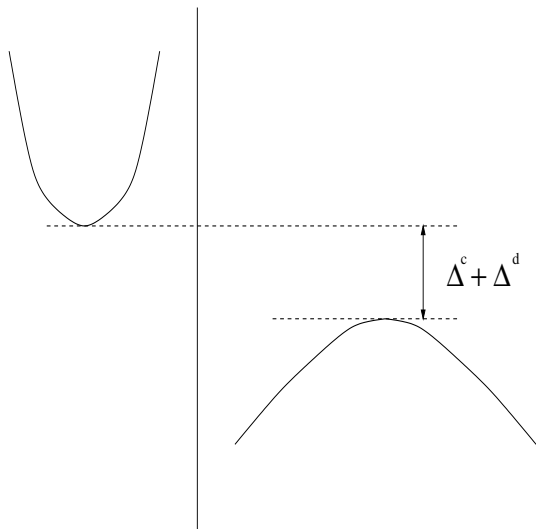


FIG. 1: Schematic diagram of band structure in the heterojunction of semiconductors.

fractionalized particle and gauge field may emerge.

Fig. 2 provides a flow chart for the development of this theory and can be used as a road-map to this paper. Starting from the microscopic Hamiltonian given by Eq. (1) we can derive a Landau theory for the order parameter χ^{ab} based on symmetry considerations. This is done in section II and the resulting Landau theory is shown in Eq. (14). Since χ^{aa} are assumed to be condensed, the remaining degrees of freedom are just $\chi^{ab} = \chi_o e^{i\theta^{ab}}$ and we focus only on phase fluctuations. Note that χ^{ab} and χ^{ba} are in general independent because χ^{ab} is the pairing of conduction electron in band a with valence hole in band b , which is distinguishable from pairing electron in band b and hole in band a . Nevertheless, due to the condensation of χ^{aa} , there is a term which locks the phases, which is proportional to $\tilde{K}_2 \sum_{a \neq b} \cos(\theta_i^{ab} + \theta_i^{ba})$. For $\tilde{K}_2 < 0$, $\theta_i^{ab} = -\theta_i^{ba}$ is favored. Thus χ^{ab} is locked to χ^{ba*} and the Landau theory reduces to a Hermitian matrix model Eq. (17). Similarly, for $\tilde{K}_2 > 0$ $\theta_i^{ab} = -\theta_i^{ba} + \pi$ is favored and we have the anti-Hermitian matrix model shown in Eq. (18). Further development depends on the next order term in χ_o . For the Hermitian model, the third order term $\tilde{K}_3 \cos(\theta_i^{ab} + \theta_i^{bc} + \theta_i^{ca})$ is allowed which leads to the constraint

$$\theta_i^{ab} + \theta_i^{bc} + \theta_i^{ca} = 0 \quad (3)$$

for strong coupling. This constraint can be satisfied by writing $\theta_i^{ab} = \phi_i^a - \phi_i^b$. The field $e^{i\phi_i^a}$ emerges as the boson field which carries the flavor quantum number, but it is coupled to a U(1) gauge field. In $d = 3$ and for large enough N , a deconfined phase is possible. It is called the Coulomb phase, because it mimics our world of non-compact QED coupled to charged particles. The Coulomb phase lies between the confined phase and the Higgs phase as a function of coupling constant κ (see Fig.

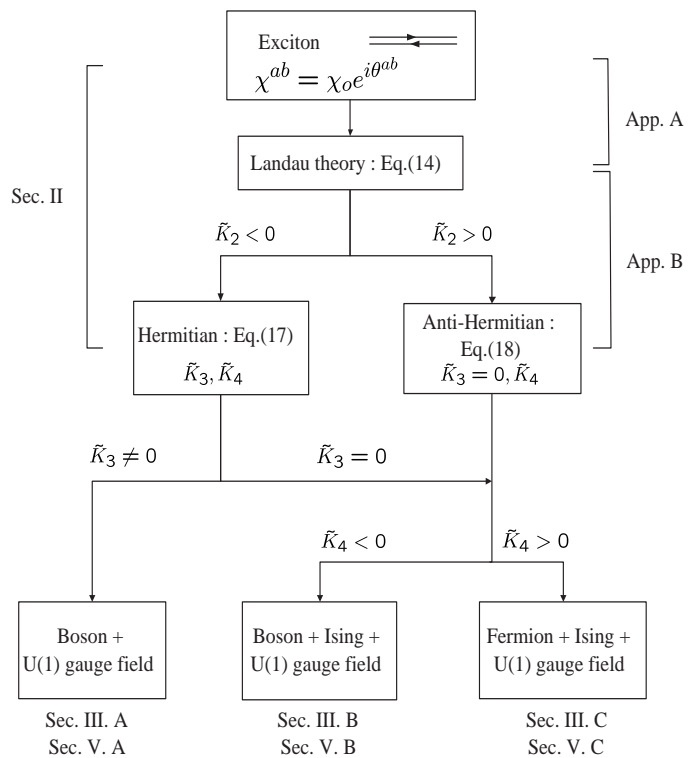


FIG. 2: Flow chart from the microscopic exciton model to low energy theories showing various fractionalized phases.

3 (a)). The Higgs phase is the phase where the off diagonal excitons are condensed and the confined phase is one where the excitons are disordered by phase fluctuations, with exponentially decaying correlation functions. The Coulomb phase is the novel phase which exhibits gapped fractionalized bosons and gapless U(1) gauge field which are analogs of photons. This is discussed in section III.A.

In section V. A we discuss this model again using the world-line representation. It is natural that the off diagonal exciton χ^{ab} is represented by a double line with a, b labels. In the strong coupling limit, these excitons scatter with each other and exchange partners rapidly (see Figs. 4 and 5). Thus the individual exciton loses its identity on a short scale ξ_1 . However, a single line carrying a flavor index may survive over a long scale ξ_2 , as shown in Fig. 6. These single lines represent the world lines of the fractionalized particles. However, it is clear that these world lines are not freely propagating, but connected to each other via a web representing multiple scattering with other excitons. The web of excitons turn out to show the same dynamics as the world sheet swept out by a line of electric flux in a compact U(1) gauge theory. This is reviewed in section IV. The size of the web gives rise to a third length scale ξ_3 shown in Fig. 6. The divergence of ξ_3 signals the transition between the confined phase and the Coulomb (deconfined) phase. Finally the divergence of ξ_2 leads to the Higgs phase of the coupled boson-gauge field system, which corresponds to the Bose condensation of the original off diagonal excitons.

Next we turn to the anti-Hermitian model, where $\tilde{K}_3 = 0$ by symmetry. The next most important term is $\tilde{K}_4 \cos(\theta_i^{ab} + \theta_i^{bc} + \theta_i^{cd} + \theta_i^{da})$. For $\tilde{K}_4 < 0$ the term favors

$$\theta_i^{ab} + \theta_i^{bc} + \theta_i^{cd} + \theta_i^{da} = 0. \quad (4)$$

These constraints are less restrictive than Eq. (3). However the set of equations (4) are not independent and it can be shown that they are satisfied by

$$\theta_i^{ab} = \phi_i^a - \phi_i^b + \frac{\pi}{2}(1 + z_i), \quad (5)$$

where $z_i = \pm 1$ is an Ising degree of freedom on each site. The resulting theory consists of the boson $e^{i\phi_i^a}$ coupled to a U(1) gauge field plus an Ising degree of freedom which is decoupled at low energies, as shown in section III.B. The world line version is discussed in Sec. V. B.

Finally for $\tilde{K}_4 > 0$, the constraint

$$\theta_i^{ab} + \theta_i^{bc} + \theta_i^{cd} + \theta_i^{da} = \pi \quad (6)$$

can not be satisfied by any bosonic parameterization. This leads to a frustration among the phases which suppresses the condensation of off diagonal excitons. However, a fermionic decomposition satisfy the constraint perfectly. A U(1) gauge field is also generated, but it turns out that a background π -flux is the favored saddle point. This leads to the familiar Dirac fermions centered at $(\pm\frac{\pi}{2}, \pm\frac{\pi}{2})$. The low energy fermion degrees of freedom is represented by a four component Dirac field, which can be interpreted as carrying spin degree of freedom, in agreement with the spin-statistics theorem. This is detailed in section III. C. It turns out that the fermion also emerges from the world line picture, because we can show that each closed loop of single world line is associated with a minus sign, as is shown in section V. C. However, the spinor nature of the fermion requires a description of the short distance physics which is not easy to capture in the world line picture.

The readers who are interested only in the low energy physics of the phenomenological model may skip the first part of Sec. II and start from the Landau model, (14). The readers who are familiar with the dual representation of the compact U(1) gauge theory may skip the Sec. IV. Sec. III and Sec. V deal with the same phenomena in two complimentary approaches. Sec. III provides a more quantitative but abstract analysis of the phenomenon of fractionalization. Sec. V is less quantitative but more physical insights can be obtained on what is really occurring in the original exciton language.

II. EFFECTIVE THEORY OF EXCITON BOSE CONDENSATE

Starting from Eq. (1), we treat the attraction between the conduction electron and the valence hole by a Hubbard-Stratonovich decoupling. The effective action

for the exciton condensate and the fermions are obtained to be (for details, see Appendix A),

$$S = S_1 + S_2, \quad (7)$$

where

$$\begin{aligned} S_1 = & \int d\tau \sum_k \sum_a \left[c_k^{a*} (\partial_\tau + \epsilon_k^c - \mu) c_k^a \right. \\ & \left. + d_k^{a*} (\partial_\tau + \epsilon_k^d - \mu) d_k^a \right] \\ & + V \sum_q \sum_{a,b} \left((\chi_q^\dagger)^{ab} \chi_q^{ba} - \frac{1}{\sqrt{v}} \sum_k c_{k+q}^{a*} \chi_q^{ab} d_k^b \right. \\ & \left. - \frac{1}{\sqrt{v}} \sum_k d_k^{b*} (\chi_q^\dagger)^{ba} c_{k+q}^a \right), \quad (8) \end{aligned}$$

and

$$\begin{aligned} S_2 = & \int d\tau \left[-\frac{VV'}{V+V'} \sum_q \sum_a |\chi_q^{aa}|^2 \right. \\ & \left. + \sqrt{v} \frac{VU}{V+V'} \sum_a (\chi_0^{aa} + \chi_0^{aa*}) \right]. \quad (9) \end{aligned}$$

Here χ_k is the $N \times N$ complex matrix for the exciton condensate field in momentum space. Each component χ_k^{ab} describes the condensate of excitons made of particle in the a -th band and hole in the b -th band. (Note that order of indices are important, $\chi^{ab} \neq \chi^{ba}$.) Self-consistent equations are solved for χ^{ab} . Various solutions are possible depending on the values of the V , V' and U . In Appendix A, a few saddle point solutions are obtained for $N = 3$. In the following we concentrate on one of the solutions,

$$\chi^{ab} = \chi_o + (\chi_d - \chi_o)\delta_{ab}, \quad (10)$$

where both the diagonal and off-diagonal components have finite amplitude.

With the exciton condensation the single particle excitation gap becomes larger than the bare band gap because it takes extra energy in breaking the particle-hole binding. At energy far below the single particle excitation gap the fluctuations of the exciton bose condensates become effective degrees of freedom. Integrating out the fermions we obtain the effective action for the exciton condensate fields χ . Symmetry enables us to construct the low energy theory without actual calculation. Since the fermions appear only in S_1 the symmetry of S_1 determines the form of the action generated by their integration. S_1 is invariant under global $U(N) \times U(N)$ transformation,

$$\begin{aligned} c_k & \rightarrow U c_k, \\ d_k & \rightarrow V d_k, \\ \chi_k & \rightarrow U \chi_k V^\dagger, \quad (11) \end{aligned}$$

where $c_k^T = (c_k^1, c_k^2, \dots, c_k^N)$, $d_k^T = (d_k^1, d_k^2, \dots, d_k^N)$ are N -component vectors for the fermion fields and \mathcal{U} and \mathcal{V} are independent $U(N)$ matrices. The symmetry put stringent constraint on possible term in the effective action because it must be invariant under the last line in Eq. (11). Up to the sixth order we write the resulting effective action,

$$\begin{aligned} \tilde{S}_1 = & \sum_{\mathbf{i}} \int d\tau \left[k_\tau \text{tr} \chi_{\mathbf{i}}^\dagger \partial_\tau \chi_{\mathbf{i}} - k \sum_{\hat{r}=\hat{1}, \dots, \hat{d}} \text{tr} (\chi_{\mathbf{i}+\hat{r}}^\dagger \chi_{\mathbf{i}} + h.c.) \right. \\ & + k_2 \text{tr} \chi_{\mathbf{i}}^\dagger \chi_{\mathbf{i}} + k'_4 (\text{tr} \chi_{\mathbf{i}}^\dagger \chi_{\mathbf{i}})^2 + k_4 \text{tr} \chi_{\mathbf{i}}^\dagger \chi_{\mathbf{i}} \chi_{\mathbf{i}}^\dagger \chi_{\mathbf{i}} \\ & + k_6 \text{tr} \chi_{\mathbf{i}}^\dagger \chi_{\mathbf{i}} \chi_{\mathbf{i}}^\dagger \chi_{\mathbf{i}} \chi_{\mathbf{i}}^\dagger \chi_{\mathbf{i}} + k'_6 (\text{tr} \chi_{\mathbf{i}}^\dagger \chi_{\mathbf{i}}) (\text{tr} \chi_{\mathbf{i}}^\dagger \chi_{\mathbf{i}} \chi_{\mathbf{i}}^\dagger \chi_{\mathbf{i}}) \\ & \left. + k''_6 (\text{tr} \chi_{\mathbf{i}}^\dagger \chi_{\mathbf{i}})^3 \right]. \end{aligned} \quad (12)$$

Here $\chi_{\mathbf{i}}$ is the exciton condensate field at space coordinate \mathbf{i} . \hat{r} is a unit vector in the d -dimensional square (cubic) lattice for $d = 2$ ($d = 3$). In principle, all of the parameters k_τ , k and k_n can be determined from the Hamiltonian (1). Note that there is only linear derivative in the imaginary time direction because the exciton is non-relativistic boson. It is convenient to discretize the imaginary time direction to rewrite the above action as

$$\begin{aligned} \tilde{S}_1 = & \sum_i \left[-\frac{K}{2} \text{tr} \chi_{i+\Delta\tau}^\dagger \chi_i - \frac{K}{4} \sum_{\hat{r}} \text{tr} (\chi_{i+\hat{r}}^\dagger \chi_i + c.c.) \right. \\ & + K_2 \text{tr} \chi_i^\dagger \chi_i + K'_4 (\text{tr} \chi_i^\dagger \chi_i)^2 + K_4 \text{tr} \chi_i^\dagger \chi_i \chi_i^\dagger \chi_i \\ & + K_6 \text{tr} \chi_i^\dagger \chi_i \chi_i^\dagger \chi_i \chi_i^\dagger \chi_i + K'_6 (\text{tr} \chi_i^\dagger \chi_i) (\text{tr} \chi_i^\dagger \chi_i \chi_i^\dagger \chi_i) \\ & \left. + K''_6 (\text{tr} \chi_i^\dagger \chi_i)^3 \right]. \end{aligned} \quad (13)$$

Here $i = (\tau, \mathbf{i})$ is index for lattice point in D -dimensional Euclidean space-time. The dimensionless coupling constants in the lattice action are given by $\tilde{K} = 2k_\tau$, $K_2 = \Delta\tau k_2 + k_\tau$ and $K_n = \Delta\tau k_n$, where the discrete time step is set to be $\Delta\tau = \frac{K}{4k}$.

The term S_2 in Eq. (9) has lower symmetry. The first term is proportional to V' which distinguishes between the interaction between particles with the same and different flavor indices. The $U(N) \times U(N)$ symmetry is broken down to $U(1)^{2N}$ where each $U(1)$ is generated by diagonal $U(N)$ matrices \mathcal{U} and \mathcal{V} , i.e., $\mathcal{U}_{ab} = \delta_{ab} e^{i\phi^a}$ and $\mathcal{V}_{ab} = \delta_{ab} e^{i\psi^a}$. The second term is proportional to U which explicitly break the phase symmetry of the diagonal exciton condensate. This further breaks the symmetry down to $U(1)^N$ where each $U(1)$ is generated by the diagonal matrix $\mathcal{U} = \mathcal{V}$. In discrete space time the total action is easily written as

$$\tilde{S} = \tilde{S}_1 + \tilde{S}_2, \quad (14)$$

$$\tilde{S}_2 = \sum_i \left[-K_{V'} \sum_a |\chi_i^{aa}|^2 + K_U \sum_a (\chi_i^{aa} + \chi_i^{aa*}) \right], \quad (15)$$

where $K_{V'} = \frac{VV'}{V+V'} \Delta\tau$ and $K_U = \frac{VU}{V+V'} \Delta\tau$.

The $U(1)^N$ transformation rotates only the phase of each component χ^{ab} . (Strictly speaking, the action (14) has only $U(1)^{N-1}$ symmetry because χ itself is invariant under one $U(1)$ transformation with $\mathcal{U} = \mathcal{V} = e^{i\phi}$.) Thus all amplitude fluctuations of χ^{ab} are gapped and we ignore the amplitude fluctuations. With the nonzero amplitudes for all exciton fields at the saddle point (10), we have N^2 independent $U(1)$ phase modes. The phases of the N diagonal modes χ^{aa} are fixed by the explicit symmetry breaking term K_U . Thus the fluctuations of the diagonal modes are gapped. Alternatively, in the case where the symmetry breaking of the diagonal excitons is spontaneous and $U = 0$, there will be N Goldstone modes. In the following we will focus on the dynamics of the remaining $N^2 - N$ off-diagonal modes which will be the same in both cases.

The effective action for the off-diagonal modes can be readily obtained from the full action (14). The phase locking of the diagonal modes plays two important roles here. First, it create mass for some of the off-diagonal modes. We pick out terms in Eq. (14) which are proportional to χ_o^2 and products of the the diagonal elements $\bar{\chi}^{aa}$. The derivation is straightforward and only the results are shown here (for details see Appendix B). This is analogous to the Higgs mechanism. Depending on the sign of the 'mass' term for the off-diagonal modes,

$$\tilde{K}_2 \sum_{a \neq b} \chi^{ab} \chi^{ba} = \tilde{K}_2 \chi_o^2 \sum_{a \neq b} \cos(\theta^{ab} + \theta^{ba}) \quad (16)$$

with $\tilde{K}_2 \equiv 2\chi_d^2 \left[K_4 + NK'_6 (\chi_d^2 + (N-1)\chi_o^2) + 3K_6 \chi_d^2 \right]$, χ is constrained to be either Hermitian or anti-Hermitian at low energy. Second, the coherent diagonal modes make the dynamics of the off diagonal mode relativistic. Once χ is constrained to be Hermitian or anti-Hermitian matrix, the excitons χ^{ab} and χ^{ba} are no longer independent, but they are anti-particles to each other. The physical picture is that two excitons χ^{ab} and χ^{ba} scatter with each other to become two diagonal excitons χ^{aa} and χ^{bb} . The diagonal excitons are condensed into vacuum and from the point of view of the off diagonal excitons, this is an annihilation process of two excitons. Conversely, two off diagonal excitons can be created out of vacuum. Since the low energy theory is relativistic, the effective action has symmetric form in space and time directions. It reduces to a Hermitian matrix model (for details see Appendix B),

$$S = -\frac{K}{4} \sum_{\langle i, j \rangle} \text{tr}' (\chi_i^\dagger \chi_j + h.c.) + \sum_{n \geq 3} \tilde{K}_n \sum_i \text{tr}' \chi_i^n \quad (17)$$

for $\tilde{K}_2 < 0$ or an anti-Hermitian matrix model,

$$S = -\frac{K}{4} \sum_{\langle i, j \rangle} \text{tr}' (\chi_i^\dagger \chi_j + h.c.) + \sum_{n \geq 2} \tilde{K}_{2n} \sum_i \text{tr}' \chi_i^{2n} \quad (18)$$

for $\tilde{K}_2 > 0$. Here i, j are indices for lattice in D-dimensional Euclidean space-time. χ is Hermitian (anti-Hermitian) matrix without diagonal element in (17) ((18)). The ' sign in the trace is to recall that there is no diagonal element in χ . The explicit form of \tilde{K}_n is also obtained in the Appendix B. The first term in the above actions is the kinetic energy term for the exciton condensate and the second term, the potential energy term.

Some remarks are in order for these models. First, (17) and (18) are two different theories in general. However they are equivalent in some special cases. The Hermitian matrix model with $\tilde{K}_{2n-1} = 0$ and $\tilde{K}_{2n} = k_{2n}$ is equivalent to the anti-Hermitian matrix model with $\tilde{K}_{2n} = (-1)^n k_{2n}$. They are related to each other by the transformation $\chi' = i\chi$. Similar equivalence also exist within the Hermitian matrix model. The Hermitian matrix model with \tilde{K}_n is equivalent to the Hermitian matrix model with $\tilde{K}'_n = (-1)^n \tilde{K}_n$. They are related by the transformation $\chi' = -\chi$. Second, the lowest order nonzero interaction is most important in the second terms of (17) and (18) if $\chi_o \ll 1$. This is because the effective phase stiffness for the off-diagonal modes is suppressed by factor of χ_o^n . More precisely, nonzero \tilde{K}_l with smallest l determines the dynamics of the theories if $|\tilde{K}_l| \gg \chi_o^m |\tilde{K}_{l+m}|$ for all m . The above consideration greatly reduces the number of theories to consider. Up to the quartic order, we have only the following three different low energy theories,

- A. Hermitian matrix model with $K_3 \neq 0$
 - B. anti-Hermitian matrix model with $K_4 < 0$ (equivalently, Hermitian matrix model with $K_3 = 0$ and $K_4 < 0$)
 - C. anti-Hermitian matrix model with $K_4 > 0$ (equivalently, Hermitian matrix model with $K_3 = 0$ and $K_4 > 0$)
- (19)

In this paper we examine the low energy physics of the above three cases in detail. We note that the cases in parenthesis in cases B and C are non-generic and require some tuning parameter to set $\tilde{K}_3 = 0$. We do not consider non-generic cases with $K_3 = K_4 = 0$ where more low energy degrees of freedom may emerge.

III. EMERGENT U(1) GAUGE THEORY IN THE MATRIX MODELS

In this section we will analyze the low energy physics of the three theories (19) in the strong coupling limit $|\tilde{K}_n| \chi_o^n \gg 1$. The degrees of freedom of the (anti) Hermitian matrix will be further reduced by the dynamical constraints imposed by the strong interaction. We will see that the low energy degrees of freedom are U(1) gauge

field and particles which carry only fractional quantum number of exciton. The statistics and spin of the fractionalized particle will be determined by the coupling constants.

A. Emergence of fractionalized boson and U(1) gauge field

Here we consider the first case in (19) : the Hermitian matrix model (17) with $\tilde{K}_3 \neq 0$. Without loss of generality we assume $\tilde{K}_3 < 0$. For simplicity we consider the case with $\tilde{K}_n < 0$ for all n even though only the \tilde{K}_3 is important for small χ_o . The \tilde{K}_3 term in (17),

$$\tilde{K}_3 \chi_o^3 \sum_{a,b,c} \cos(\theta^{ab} + \theta^{bc} + \theta^{ca}) \quad (20)$$

leads to constraints (in addition to the Hermitivity),

$$\theta^{ab} + \theta^{bc} + \theta^{ca} = 0 \quad (21)$$

in the strong coupling limit $|\tilde{K}_3| \chi_o^3 \gg 1$. These conditions also constrain sum of $n \geq 4$ phases. For example, by summing the two conditions

$$\begin{aligned} \theta^{ab} + \theta^{bc} + \theta^{ca} &= 0, \\ \theta^{ac} + \theta^{cd} + \theta^{da} &= 0 \end{aligned} \quad (22)$$

and using the Hermitivity $\theta^{ca} + \theta^{ac} = 0$, we obtain

$$\theta^{ab} + \theta^{bc} + \theta^{cd} + \theta^{da} = 0. \quad (23)$$

Thus the higher order interaction terms in (17) are also minimized with $\tilde{K}_n < 0$. The number of independent constraints imposed by (21) is $\frac{(N-1)(N-2)}{2}$ [22]. leading to $\frac{N(N-1)}{2} - \frac{(N-1)(N-2)}{2} = N - 1$ soft modes. These modes can be parametrized by the N phases ϕ^a so that

$$\theta_i^{ab} = \phi_i^a - \phi_i^b \quad (24)$$

with a redundancy $\phi_i^a \sim \phi_i^a + \phi_i$. The (N-1) low energy bosons are the soft modes associated with the $U(1)^{N-1}$ symmetry of the Landau theory (14). Note that $e^{i\phi_i^a}$ carries only one flavor quantum number while exciton carries two. Thus we refer to this boson as *fractional* boson. At this stage, the fractional boson is just a book-keeping tool. It may or may not appear as low energy excitation. If the fractional boson appears as true low energy excitation, we will refer to it as *fractionalized* boson, the term which is mainly used in literatures.

For the low energy modes ϕ_i^a there is no potential energy since Eq. (20) is minimized. The effective action becomes

$$S = -\frac{\kappa}{4} \sum_{a < b} \sum_{\langle i, j \rangle} \left[e^{i(\phi_i^a - \phi_j^a)} e^{-i(\phi_i^b - \phi_j^b)} + c.c. \right], \quad (25)$$

where $\kappa = 2K\chi_o^2$. Introducing the Hubbard-Stratonovich transformation for the quartic term,

$$\begin{aligned} & \exp\left(\frac{\kappa}{4}e^{i(\phi_i^a-\phi_j^a)}e^{i(\phi_j^b-\phi_i^b)} + c.c.\right) \\ &= \left(\frac{\kappa}{4\pi}\right)^2 \int d\eta_{ij}^{ab} d\eta_{ij}^{ab*} d\eta_{ji}^{ab} d\eta_{ji}^{ab*} \\ & \times \exp\left(-\frac{\kappa}{4}\left[|\eta_{ij}^{ab}|^2 + |\eta_{ji}^{ab}|^2\right.\right. \\ & \left.-\eta_{ij}^{ab}e^{i(\phi_i^a-\phi_j^a)} - \eta_{ij}^{ab*}e^{i(\phi_j^b-\phi_i^b)}\right. \\ & \left.-\eta_{ji}^{ab}e^{-i(\phi_i^a-\phi_j^a)} - \eta_{ji}^{ab*}e^{-i(\phi_j^b-\phi_i^b)}\right]\right), \quad (26) \end{aligned}$$

and parameterizing the two complex Hubbard-Stratonovich fields by four real variables,

$$\begin{aligned} \eta_{ij}^{ab} &= |\tilde{\eta}_{ij}^{ab}|e^{w_{ij}^{ab}+i(a_{ij}^{+ab}-a_{ij}^{ab})}, \\ \eta_{ji}^{ab} &= |\tilde{\eta}_{ij}^{ab}|e^{-w_{ij}^{ab}+i(a_{ij}^{+ab}+a_{ij}^{ab})}, \end{aligned} \quad (27)$$

we obtain the action

$$\begin{aligned} S_b &= \frac{\kappa}{4} \sum_{\langle i,j \rangle, a < b} \left[2|\tilde{\eta}_{ij}^{ab}|^2 \cosh(2w_{ij}^{ab}) \right. \\ & \left. - |\tilde{\eta}_{ij}^{ab}|e^{w_{ij}^{ab}+i(a_{ij}^{+ab}-a_{ij}^{ab})}e^{i(\phi_i^a-\phi_j^a)} \right. \\ & \left. - |\tilde{\eta}_{ij}^{ab}|e^{-w_{ij}^{ab}+i(a_{ij}^{+ab}+a_{ij}^{ab})}e^{-i(\phi_i^a-\phi_j^a)} \right. \\ & \left. - |\tilde{\eta}_{ij}^{ab}|e^{w_{ij}^{ab}+i(-a_{ij}^{+ab}+a_{ij}^{ab})}e^{i(\phi_j^b-\phi_i^b)} \right. \\ & \left. - |\tilde{\eta}_{ij}^{ab}|e^{-w_{ij}^{ab}+i(-a_{ij}^{+ab}-a_{ij}^{ab})}e^{-i(\phi_j^b-\phi_i^b)} \right]. \quad (28) \end{aligned}$$

Among the auxiliary fields, there is only one massless modes associated with the U(1) gauge symmetry,

$$\begin{aligned} \phi_i^a &\rightarrow \phi_i^a + \varphi_i, \\ a_{ij}^{ab} &\rightarrow a_{ij}^{ab} + \varphi_i - \varphi_j. \end{aligned} \quad (29)$$

We retain the U(1) gauge field and neglect the fluctuations of other auxiliary fields. In general the action (28) is not real but reality is restored at the saddle point where a_{ij}^{+ab} and w_{ij}^{ab} have saddle points in the imaginary direction[23]. In our case, by comparing the first and last terms in Eq. (28), we note that the only solution where the effective hopping is the same for all species of bosons is

$$a_{ij}^{+ab'} = w_{ij}^{ab} = 0. \quad (30)$$

The massless mode is one where a_{ij}^{ab} is independent of the flavor index, i.e., $a_{ij}^{ab} = a_{ij}$ and the low energy action becomes

$$S_b = \frac{\kappa}{4}(N-1) \sum_a \sum_{\langle i,j \rangle} \left[\eta^2 - \eta e^{i(\phi_i^a-\phi_j^a-a_{ij})} - c.c. \right], \quad (31)$$

where $|\tilde{\eta}_{ij}^{ab}| = \eta$. This is the familiar problem of compact U(1) gauge theory coupled with N bosons. The

bare gauge coupling is infinite. At low energy the gauge coupling is renormalized to be finite. For example, by expanding in κ and integrating out bosons which hop around a plaquette, we produce a gauge coupling associated with the Maxwellian term on the unit plaquette in the D-dimensional (hyper) cubic lattice, $g^2 \sim \frac{1}{t^{\frac{1}{N}}}$ with $t \equiv \frac{\kappa}{4}(N-1)\eta$. In the small g limit the confinement phase occurs. The fractional bosons do not appear as excitation. All excitations are gapped. This is the disordered phase of the off diagonal excitons. In the large t limit the bosons have phase coherence (Higgs phase). One of the N boson is eaten by the massive U(1) gauge field. There are remaining $N-1$ massless modes. In terms of original exciton, this is the phase where the $N^2 - N$ off diagonal excitons are bose condensed. Due to locking with the already correlated diagonal excitons, only $N-1$ modes survive as the Goldstone modes associated with the off diagonal exciton condensates. This is the expected result from the $U(1)^{N-1}$ symmetry as discussed in Sec. II. These are the possible phases in (2+1)-dimension. In higher dimension the Coulomb phase can occur between the confinement and Higgs phases. In the Coulomb phase the photon emerges as a massless collective excitation of excitons. The physical meaning of the photon in terms of original exciton will be discussed in the Sec. V. A. In this phase the bosons are gapped and interact by exchange of photons. The schematic phase diagram in (3+1)-dimension is shown in Fig. 3 (a).

Since the fractionalized boson emerges from the exciton which is charge neutral to electromagnetic field, it is obvious that it is charge neutral as well. The fractionalized boson is structureless and it seems obvious that the boson has spin 0. By spin 0 we mean that the boson transforms trivially under Lorentz transformation in the continuum limit. However we need to take into account the coupling to the gauge field in order to determine the spin of the boson at low energy. Let us follow only one species of boson by integrating out the rest of the bosons. For small t we obtain

$$\begin{aligned} S &= -t \sum_{\langle i,j \rangle} \left[e^{i(\phi_i-\phi_j-a_{ij})} + c.c. \right] \\ & \quad - \sum_C \frac{1}{2g_C^2} \cos b_C. \end{aligned} \quad (32)$$

Here the flavor index for the remaining boson is dropped. C denotes loop in space-time traced by the integrated bosons. $b_C \equiv \oint_C a$ is the flux associated with the loop. $g_C^2 \sim \frac{1}{(N-1)t^{L(C)}}$ is the generalized gauge coupling for the non-local gauge action with $L(C)$, the length of the loop C . In the massive phase for the fractionalized boson with $t \ll 1$ small loop contributions dominate the gauge action. Note that the gauge coupling can be made small with large N even for small t . In the Coulomb phase the gauge field has the saddle point value $a_{ij} = 0$. Hence the background gauge field for the remaining boson is smoothly varying in space-time. Thus the boson remains to be structureless in the long-wavelength limit. The

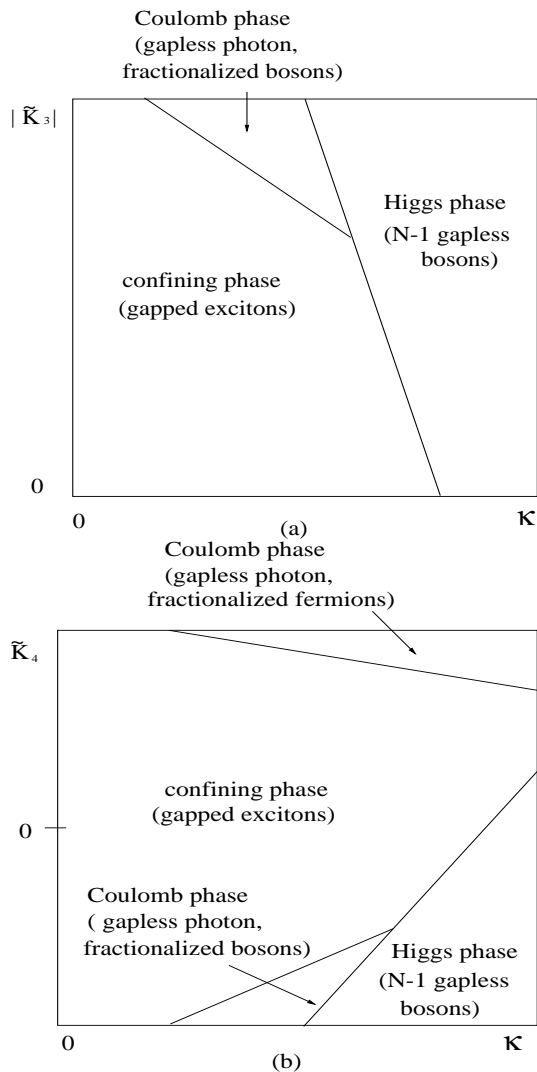


FIG. 3: Schematic phase diagrams of (a) the Hermitian matrix model with $\tilde{K}_3 \neq 0$ and (b) the anti-Hermitian matrix model (equivalently the Hermitian matrix model with $\tilde{K}_3 = 0$) in $d = 3$. The Ising transition line is not shown in (b).

continuum Lagrangian for the emergent boson becomes

$$\mathcal{L} = \sum_{\mu} \tilde{t}_{\mu} (\partial_{\mu} \phi - a_{\mu})^2 + \frac{1}{2\tilde{g}^2} \sum_{\mu, \nu} f_{\mu\nu}^2, \quad (33)$$

where \tilde{t}_{μ} and \tilde{g} are the renormalized phase stiffness and gauge coupling respectively. $f_{\mu\nu} = \partial_{\mu} a_{\nu} - \partial_{\nu} a_{\mu}$ is the field strength tensor for the emergent non-compact gauge field. The fractionalized boson is in the disordered phase due to the proliferation of vortices and emerges as gapped excitation which has the relativistic dispersion,

$$\omega_k = \sqrt{v^2 k^2 + m^2}, \quad (34)$$

where $v = \sqrt{t_1/t_0}$ is the velocity with $t_0 = \tilde{t}_{\mu=0}$, $t_1 = \tilde{t}_{\mu \neq 0}$ and m , the mass gap. The mass gap vanishes at the transition to the Higgs phase. If the background gauge

field had turned out to be rapidly varied in the lattice scale, the emergent particle in the long-wavelength limit would have been different from the boson in the lattice scale. If this were the case, multiple components which correspond to spin quantum numbers could emerge in the continuum limit from the doubling of unit cell. This turns out to be the case for emergent fermions, as we shall see later.

B. Emergence of fractionalized boson, Ising mode and U(1) gauge field

In this section we consider the second case in (19). For simplicity, we consider the Hermitian matrix model with $\tilde{K}_{2n} < 0$ for all n . Equivalently, we may use the anti-Hermitian matrix model with $\tilde{K}_{2n} = (-1)^{n-1} |\tilde{K}_{2n}|$. Here we use the Hermitian matrix model because it is more convenient to make the coupling constant have same sign. The fourth order term in (18),

$$\tilde{K}_4 \chi_o^4 \sum_{a,b,c,d} \cos(\theta^{ab} + \theta^{bc} + \theta^{cd} + \theta^{da}) \quad (35)$$

leads to the constraints

$$\theta_i^{ab} + \theta_i^{bc} + \theta_i^{cd} + \theta_i^{da} = 0 \quad (36)$$

for $|\tilde{K}_4| \chi_o^4 \gg 1$. Surprisingly, these conditions also constrain the sum of three exciton phases. By summing the three equations,

$$\begin{aligned} \theta_i^{ab} + \theta_i^{bd} + \theta_i^{dc} + \theta_i^{ca} &= 0, \\ \theta_i^{ac} + \theta_i^{cb} + \theta_i^{bd} + \theta_i^{da} &= 0, \\ \theta_i^{ad} + \theta_i^{dc} + \theta_i^{cb} + \theta_i^{ba} &= 0, \end{aligned} \quad (37)$$

and using the Hermiticity, $\theta_i^{ab} + \theta_i^{ba} = 0$, we obtain

$$2(\theta_i^{cb} + \theta_i^{bd} + \theta_i^{dc}) = 0. \quad (38)$$

Therefore the sum of three phases are fixed up to Z_2 degree of freedom,

$$\theta_i^{cb} + \theta_i^{bd} + \theta_i^{dc} = 0 \text{ or } \pi. \quad (39)$$

The constraint for the four phases (36) is less restrictive than the constraint for the three phases (21) in the previous section and an extra Z_2 degrees of freedom is needed. Thus the low energy degrees of freedom are parameterized by the N bosonic variables and a Z_2 variable,

$$\theta_i^{ab} = \phi_i^a - \phi_i^b + \frac{\pi}{2}(1 + z_i), \quad (40)$$

with $z_i = \pm 1$. The Hermiticity is satisfied with the decomposition. The \tilde{K}_{2n} term with $n \geq 3$ is also minimized because

$$\cos(\theta_i^{a_1 a_2} + \theta_i^{a_2 a_3} + \dots + \theta_i^{a_{2n} a_1}) = 1. \quad (41)$$

Thus one exciton field is decomposed into three degrees of freedom. The two U(1) phases are the same modes which appear in the previous section. The Ising mode is the flavor independent Z_2 degree of freedom. It is noted that z_i is an independent degree of freedom because it can not be absorbed into ϕ^a or ϕ^b . This can be illustrated by the relation $z_i = -e^{i(\theta^{ab} + \theta^{bc} + \theta^{ca})}$ whose value is not affected by the change of ϕ^a . The z_i describes the low energy Z_2 degree of freedom for a composite of three excitons. Another important consequence of this relation is that because z_i is fully determined in terms of θ^{ab} 's, there is no gauge symmetry under which the Z_2 variable transforms nontrivially. This is contrary to the gauge symmetry of the U(1) variables, $\phi_i^a \rightarrow \phi_i^a + \phi_i$. The structure of local symmetry in the decomposition determines how the fractional particles are coupled to emergent gauge field at low energy. There will be U(1) gauge field coupled to the U(1) fields, but no gauge coupling to the Ising mode.

The effective action for the low energy modes becomes

$$S = -\frac{\kappa}{4} \sum_{a < b} \sum_{\langle i, j \rangle} \left[e^{i(\phi_i^a - \phi_j^a)} e^{-i(\phi_i^b - \phi_j^b)} e^{i\frac{\pi}{2}(z_i - z_j)} + c.c. \right], \quad (42)$$

where $\kappa = 2K\chi_0^2$. We first decompose the U(1) variables from the Z_2 variables,

$$\begin{aligned} & \exp \left(\frac{\kappa}{4} e^{i(\phi_i^a - \phi_j^a) - i(\phi_i^b - \phi_j^b)} e^{i\frac{\pi}{2}(z_i - z_j)} + c.c. \right) \\ &= \left(\frac{\kappa}{4\pi} \right)^2 \int d\xi_{ij}^{ab} d\xi_{ij}^{ab*} d\xi_{ji}^{ab} d\xi_{ji}^{ab*} \\ & \times \exp \left(-\frac{\kappa}{4} \left[|\xi_{ij}^{ab}|^2 + |\xi_{ji}^{ab}|^2 \right. \right. \\ & \left. \left. - \xi_{ij}^{ab} e^{i(\phi_i^a - \phi_j^a) - i(\phi_i^b - \phi_j^b)} - \xi_{ij}^{ab*} e^{i\frac{\pi}{2}(z_i - z_j)} \right. \right. \\ & \left. \left. - \xi_{ji}^{ab} e^{-i(\phi_i^a - \phi_j^a) + i(\phi_i^b - \phi_j^b)} - \xi_{ji}^{ab*} e^{-i\frac{\pi}{2}(z_i - z_j)} \right] \right) \end{aligned} \quad (43)$$

With the parameterization for the Hubbard-Stratonovich fields

$$\begin{aligned} \xi_{ij}^{ab} &= |\tilde{\xi}_{ij}^{ab}| e^{x_{ij}^{ab} + i(c_{ij}^{+ab} + c_{ij}^{ab})}, \\ \xi_{ji}^{ab} &= |\tilde{\xi}_{ij}^{ab}| e^{-x_{ij}^{ab} + i(c_{ij}^{+ab} - c_{ij}^{ab})}, \end{aligned} \quad (44)$$

the action becomes

$$\begin{aligned} S &= \frac{\kappa}{4} \sum_{\langle i, j \rangle, a < b} \left[2|\tilde{\xi}_{ij}^{ab}|^2 \cosh(2x_{ij}^{ab}) \right. \\ & \left. - |\tilde{\xi}_{ij}^{ab}| e^{x_{ij}^{ab} + i(c_{ij}^{+ab} + c_{ij}^{ab})} e^{i(\phi_i^a - \phi_j^a) - i(\phi_i^b - \phi_j^b)} \right. \\ & \left. - |\tilde{\xi}_{ij}^{ab}| e^{-x_{ij}^{ab} + i(c_{ij}^{+ab} - c_{ij}^{ab})} e^{-i(\phi_i^a - \phi_j^a) + i(\phi_i^b - \phi_j^b)} \right. \\ & \left. - |\tilde{\xi}_{ij}^{ab}| e^{x_{ij}^{ab} + i(-c_{ij}^{+ab} - c_{ij}^{ab})} e^{i\frac{\pi}{2}(z_i - z_j)} \right. \\ & \left. - |\tilde{\xi}_{ij}^{ab}| e^{-x_{ij}^{ab} + i(-c_{ij}^{+ab} + c_{ij}^{ab})} e^{-i\frac{\pi}{2}(z_i - z_j)} \right]. \end{aligned} \quad (45)$$

The action is not Hermitian. However the Hermiticity is restored at the saddle point $x_{ij}^{ab} = i\tilde{x}_{ij}^{ab}$ and $c_{ij}^{+ab} = i\tilde{c}_{ij}^{+ab}$

with real \tilde{x}_{ij}^{ab} and \tilde{c}_{ij}^{+ab} . At the saddle point we have real action,

$$S = \frac{\kappa}{4} \sum_{\langle i, j \rangle, a < b} \left[\xi_z \xi_\phi - \xi_z e^{i(\phi_i^a - \phi_j^a) - i(\phi_i^b - \phi_j^b)} - \xi_\phi e^{i\frac{\pi}{2}(z_i - z_j)} \right] + c.c., \quad (46)$$

where $\xi_z \equiv |\tilde{\xi}_{ij}^{ab}| e^{-\tilde{c}_{ij}^{+ab} + i(\tilde{x}_{ij}^{ab} + c_{ij}^{ab})}$ and $\xi_\phi \equiv |\tilde{\xi}_{ij}^{ab}| e^{\tilde{c}_{ij}^{+ab} + i(\tilde{x}_{ij}^{ab} - c_{ij}^{ab})}$. All the fluctuations of the auxiliary field around the saddle point is massive. Thus the U(1) phase modes and the Ising mode are decoupled at low energy. The saddle point values of the auxiliary fields are determined from the self-consistency conditions,

$$\begin{aligned} \xi_z &= \left\langle e^{i\frac{\pi}{2}(z_i - z_j)} \right\rangle, \\ \xi_\phi &= \left\langle e^{i(\phi_i^a - \phi_j^a) - i(\phi_i^b - \phi_j^b)} \right\rangle. \end{aligned} \quad (47)$$

The solution with $\xi_z, \xi_\phi > 0$ satisfies the self-consistency. That is, positive ξ_ϕ gives $\langle e^{i\frac{\pi}{2}(z_i - z_j)} \rangle > 0$ and positive ξ_z , in turn, gives $\langle e^{i(\phi_i^a - \phi_j^a) - i(\phi_i^b - \phi_j^b)} \rangle > 0$. Thus the Z_2 variable is ferromagnetically coupled with each other. The final result is the same as that of the usual mean-field decomposition with $AB \rightarrow \langle A \rangle B + A \langle B \rangle - \langle A \rangle \langle B \rangle$. The merit of the above procedure is that one can easily identify the low energy degrees of freedom beyond the saddle point approximation[23].

The quartic term of the U(1) phase modes are decoupled by the same transformation used in the previous section. Finally, we obtain the compact U(1) gauge theory coupled with N bosons and the ferromagnetically coupled Ising field,

$$\begin{aligned} S &= -t \sum_a \sum_{\langle i, j \rangle} \left[e^{i(\phi_i^a - \phi_j^a - a_{ij})} + c.c. \right] \\ & \quad - t_z \sum_{\langle i, j \rangle} z_i z_j, \end{aligned} \quad (48)$$

where $t = \frac{\kappa}{4}(N-1)\xi_z\eta$ and $t_z = \frac{\kappa}{4}N(N-1)\xi_\phi$.

The physics of the U(1) gauge sector is the same as the one discussed in the previous section. On the other hand, the Ising variable undergoes a second order phase transition from the disordered phase to ordered phase as t_z increases. The low energy dynamics of the Ising mode is described by the real Klein-Gordon model. The energy dispersion becomes

$$\omega_k = \sqrt{v_I^2 k^2 + m_I^2}, \quad (49)$$

where v_I is the velocity and m_I , the mass gap. The mass gap vanishes only at the critical point. In the ordered phase the composite field of three excitons has long range correlation. Since the low energy theories are decoupled for the U(1) and the Ising sectors, the Ising transition can occur within any phase in the phase diagram of Fig.

3 (b). If the Ising transition occurs within the Higgs phase, the Higgs phase of the fractionalized boson without long range correlation of exciton is possible. In this phase pairs of off diagonal excitons are condensed, i.e., $\langle e^{i(\theta^{ab}+\theta^{cd})} \rangle \neq 0$. This is in contrast to case A.

C. Emergence of fractionalized fermion, Ising mode and U(1) gauge field

In this section we consider the third case in (19). Here we choose to use the anti-Hermitian matrix model with $\tilde{K}_{2n} > 0$ which is equivalent to the Hermitian matrix model with $\tilde{K}_{2n} = (-1)^n |\tilde{K}_{2n}|$. The potential energy

$$K_{2n} \text{tr}' \chi^{2n} = K_{2n} \chi_o^{2n} \sum_{a_1, \dots, a_{2n}} \cos(\theta^{a_1 a_2} + \theta^{a_2 a_3} + \dots + \theta^{a_{2n} a_1}) \quad (50)$$

is minimized when

$$\theta_i^{a_1 a_2} + \theta_i^{a_2 a_3} + \dots + \theta_i^{a_{2n} a_1} = \pi. \quad (51)$$

These become constraints if $K_{2n} \chi_o^{2n} \gg 1$. The condition (51) defines the ‘low energy valley’ in the phase space of θ^{ab} . However there is no bosonic parameterization for the low energy modes because of frustration in the interaction. This can be argued in the following ways. Firstly, (51) is not consistent with the anti-Hermitian matrix. The constraint $\theta_i^{ab} + \theta_i^{bc} + \theta_i^{cd} + \theta_i^{da} = \pi$ leads to $\theta_i^{ab} + \theta_i^{ba} + \theta_i^{bc} + \theta_i^{cb} = \pi$ for $d = b$. However this is inconsistent with the anti-Hermiticity condition $\theta_i^{ab} + \theta_i^{ba} = \pi$ which leads to $\theta_i^{ab} + \theta_i^{ba} + \theta_i^{bc} + \theta_i^{cb} = 0 \pmod{2\pi}$. Secondly, the conditions (51) are frustrated among themselves. Summing the two equations $\theta_i^{ab} + \theta_i^{bc} + \theta_i^{cd} + \theta_i^{da} = \pi$, $\theta_i^{ae} + \theta_i^{ec} + \theta_i^{cb} + \theta_i^{ba} = \pi$ and using the anti-Hermiticity $\theta_i^{ab} + \theta_i^{ba} = \pi$, $\theta_i^{bc} + \theta_i^{cb} = \pi$ we obtain $\theta_i^{cd} + \theta_i^{da} + \theta_i^{ae} + \theta_i^{ec} = 0 \pmod{2\pi}$. In other words, the set of constraint given by Eq. (51) is inherently frustrated and can not be all satisfied by any set of $\{\theta^{ab}\}$ where θ^{ab} are c-numbers.

We are thus motivated to introduce anti-commutativity,

$$e^{i\theta_i^{ab}} = i\psi_i^{a*} \psi_i^b. \quad (52)$$

Here ψ is Grassmann fields. The i is introduced to satisfy anti-Hermiticity, $e^{i\theta_i^{ba}} = -\left(e^{i\theta_i^{ab}}\right)^*$. Because of the anti-commutativity, all of the constraints can be satisfied, i.e.,

$$\begin{aligned} \langle e^{i(\theta_i^{ab} + \theta_i^{bc} + \theta_i^{cd} + \theta_i^{da})} \rangle &= \langle \psi_i^{a*} \psi_i^b \psi_i^{b*} \psi_i^c \psi_i^{c*} \psi_i^d \psi_i^{d*} \psi_i^a \rangle \\ &= -\langle \psi_i^a \psi_i^{a*} \psi_i^b \psi_i^{b*} \psi_i^c \psi_i^{c*} \psi_i^d \psi_i^{d*} \rangle \\ &= -1. \end{aligned} \quad (53)$$

Here the fermionic functional integral is performed with the measure,

$$\int \Pi_{a<b} \left[\frac{d\theta^{ab}}{2\pi} \right] = \int \Pi_a [d\psi^{a*} d\psi^a] \mathcal{M}, \quad (54)$$

$$\mathcal{M} = i^N e^{-i \sum_a \psi^a \psi^{a*}}, \quad (55)$$

where the integration in the left hand side of Eq. (54) is understood to be performed over the low energy valley in the energy landscape for the exciton phases. However the decomposition (52) is not complete yet. This is because the fermionic decomposition also predicts $\langle e^{i(\theta_i^{ab} + \theta_i^{bc} + \theta_i^{ca})} \rangle \neq 0$, while it is zero in the original exciton representation. It should be zero due to the Z_2 symmetry ($\theta_i^{ab} \rightarrow \theta_i^{ab} + \pi$) of the action (18). Thus we include the extra Z_2 degree of freedom,

$$e^{i\theta_i^{ab}} = i\psi_i^{a*} \psi_i^b e^{i\frac{\pi}{2}(1+z_i)}, \quad (56)$$

with $z_i = \pm 1$. The situation is similar to the bosonic case in the previous section.

With the decomposition we have the consistency for elementary integrations,

$$\begin{aligned} \langle 1 \rangle &= \frac{1}{2} \sum_z \int \Pi_a [d\psi^{a*} d\psi^a] \mathcal{M} = 1, \\ \langle e^{i\theta^{bc}} \rangle &= \frac{1}{2} \sum_z \int \Pi_a [d\psi^{a*} d\psi^a] \mathcal{M} i z \psi^{b*} \psi^c = 0, \\ \langle e^{i\theta^{bc}} e^{-i\theta^{bc}} \rangle &= \frac{1}{2} \sum_z \int \Pi_a [d\psi^{a*} d\psi^a] \mathcal{M} \psi^{b*} \psi^c \psi^{c*} \psi^b = 1, \end{aligned} \quad (57)$$

and the potential energy is minimized,

$$\langle \cos(\theta_i^{a_1 a_2} + \theta_i^{a_2 a_3} + \dots + \theta_i^{a_{2n} a_1}) \rangle = -1 \quad (58)$$

for all $\{a_1, a_2, \dots, a_{2n}\}$. At the same time the product of odd number of exciton fields has zero expectation value because of the fluctuating Z_2 degree of freedom. This is also consistent with the property of original field. Thus these fermionic variables and the Z_2 spins are the low energy modes of the system in the strong coupling regime. Note that the fermionic decomposition is over-estimating the expectation value of potential energy because the absolute value of the left hand side in Eq. (58) should be less than 1. For a quantitative agreement one may have to introduce four or higher fermion terms in the measure. Here we proceed with the measure (55) because the four or higher fermion interaction is irrelevant at low energy for $d \geq 2$.

The partition function is written as

$$Z = \int \sum_z \Pi_{i,a} (i d\psi_i^{a*} d\psi_i^a) e^{-S}, \quad (59)$$

where

$$\begin{aligned} S &= i \sum_i \sum_a \psi_i^a \psi_i^{a*} \\ &+ \frac{\kappa}{4} \sum_{a<b} \sum_{\langle i,j \rangle} \left[\psi_i^{a*} \psi_j^a \psi_j^{b*} \psi_i^b e^{i\frac{\pi}{2}(z_i - z_j)} + c.c. \right] \end{aligned} \quad (60)$$

with $\kappa = 2K\chi_o^2$. The measure of the integration can be cast into the conventional form by the

transformation[24].

$$\begin{aligned}\psi_i^a &= e^{i\frac{\pi}{4}}\psi_i^{a'}, \\ \psi_i^{a*} &= e^{i\frac{\pi}{4}}\psi_i^{a'*}.\end{aligned}\quad (61)$$

Note that this transformation does not respect the original ‘complex conjugacy’ of ψ_i^a and ψ_i^{a*} . However it is legitimate because $\psi_1 \equiv \psi_i^a$ and $\psi_2 \equiv \psi_i^{a*}$ can be regarded as two independent Grassmann variables. The partition function in the transformed fields becomes,

$$Z = \int \sum_z \Pi_{i,a} \left(d\psi_i^{a'*} d\psi_i^{a'} \right) e^{-S}, \quad (62)$$

with the action

$$\begin{aligned}S &= -\sum_a \sum_i \psi_i^{a'} \psi_i^{a'*} \\ &\quad -\frac{\kappa}{4} \sum_{a<b} \sum_{\langle i,j \rangle} \left[\psi_i^{a'*} \psi_j^{a'} \psi_j^{b'*} \psi_i^{b'} e^{i\frac{\pi}{2}(z_i - z_j)} + c.c. \right]\end{aligned}\quad (63)$$

In the following we will drop ‘prime’ sign in $\psi_i^{a'}$. The procedure of decomposing the Z_2 spin and the fermionic variables is exactly the same as the bosonic case in the previous section. The final low energy action is obtained to be two decoupled theories,

$$\begin{aligned}S &= \sum_a \sum_i \psi_i^{a*} \psi_i^a - t \sum_a \sum_{\langle i,j \rangle} \left[e^{ia_{ij}} \psi_i^{a*} \psi_j^a + c.c. \right] \\ &\quad -t_z \sum_{\langle i,j \rangle} z_i z_j.\end{aligned}\quad (64)$$

The Ising variable can have disordered and ordered phases as discussed in Sec. III. B. In the following we focus on the fermions coupled with the compact $U(1)$ gauge field. Note that this fermion is spinless (structureless). The spin-statistics theorem does not apply here because there is no full Lorentz invariance in lattice. It is in the long wavelength limit much larger than the lattice scale where the spin-statistics theorem requires half integer spin for the fermion because of the full Lorentz invariance. In the following we will see how the fermion acquires spin at low energy. Similarly to the bosonic case, we focus on one species of fermion by integrating out the rest of fermions. We obtain the effective action for the gauge field,

$$\begin{aligned}S &= \sum_i \psi_i^* \psi_i - t \sum_{\langle i,j \rangle} \left[e^{ia_{ij}} \psi_i^* \psi_j + c.c. \right] \\ &\quad + \sum_C \frac{1}{2g_C^2} \cos b_C.\end{aligned}\quad (65)$$

$b_C \equiv \oint_C a$ is the flux associated with the loop C . $g_C^2 \sim \frac{1}{(N-1)tL(C)}$ is the generalized gauge coupling for the non-local gauge action with $L(C)$, the length of the loop C . Note that the sign of the gauge action is opposite to the

one obtained from the bosonic action (65). The difference in sign comes from the difference in the statistics of the integrated matters. This difference in statistics makes the difference in the low energy spin structure, confirming the spin-statistics theorem.

In the small t limit, the unit plaquette term is most important in the gauge kinetic energy term. Because of the opposite sign in the gauge kinetic energy term, the saddle point of (65) is ‘ π -flux’ phase where every space-time plaquette encloses flux π . Now we derive the low energy theory for the fermion in $2+1D$. Generalization to higher dimension is straightforward. For the ‘ π -flux’, it is convenient to work in a unit cell which is doubled in both the x and y directions, but not the z direction, with the gauge choice

$$\begin{aligned}a_{r+x,r} &= i, \\ a_{r+y,r} &= (-1)^{r_x+r_y}, \\ a_{r+z,r} &= i(-1)^{r_x+r_y}.\end{aligned}\quad (66)$$

The above ‘ π -flux’ has been used in lattice gauge theory to put Dirac fermion in lattice using only one-component fermion[25]. The difference from the Ref. [25] is that in our case the z direction is the imaginary time direction. More importantly in our case the ‘ π -flux’ is the dynamical consequence while it is assumed in Ref. [25]. In the ‘ π -flux’ phase the action for the remaining fermion becomes

$$\begin{aligned}S &= \sum_I \sum_{A=1}^4 \psi_{IA}^* \psi_{IA} \\ &\quad -t \sum_I \left[i\psi_{I2}^* \psi_{I1} - \psi_{I3}^* \psi_{I2} - i\psi_{I4}^* \psi_{I3} + \psi_{I1}^* \psi_{I4} \right. \\ &\quad \left. + i\psi_{I+x1}^* \psi_{I2} + i\psi_{I+x4}^* \psi_{I3} + \psi_{I+y2}^* \psi_{I3} - \psi_{I+y1}^* \psi_{I4} \right. \\ &\quad \left. + i\psi_{I+z1}^* \psi_{I1} - i\psi_{I+z2}^* \psi_{I2} + i\psi_{I+z3}^* \psi_{I3} - i\psi_{I+z4}^* \psi_{I4} \right] \\ &\quad -c.c.,\end{aligned}\quad (67)$$

where I is the unit cell index and $A = 1, 2, 3, 4$ labels the sites within a unit cell. Introducing four-component ‘spinor’, $\bar{\Psi}_I = (\psi_{I1}^*, \psi_{I2}^*, \psi_{I3}^*, \psi_{I4}^*)$, $\Psi_I^T = (\psi_{I1}, \psi_{I2}, \psi_{I3}, \psi_{I4})$, the action is written

$$\begin{aligned}S &= \sum_I \bar{\Psi}_I \left[\hat{I} - t \begin{pmatrix} -2i\Delta_z & -i\Delta_x & 0 & \Delta_y \\ -i\Delta_x & 2i\Delta_z & -\Delta_y & 0 \\ 0 & \Delta_y & -2i\Delta_z & -i\Delta_x \\ -\Delta_y & 0 & -i\Delta_x & 2i\Delta_z \end{pmatrix} \right] \Psi_I \\ &\quad + O(\Delta^2),\end{aligned}\quad (68)$$

where \hat{I} is identity matrix and $\Delta_p \Psi_I = \Psi_{I+p} - \Psi_I$. We rescale the coordinates $\Delta_x \rightarrow \partial_x$, $\Delta_y \rightarrow \partial_y$, $2\Delta_z \rightarrow \partial_z$ in the continuum limit. Introducing a new basis

$$\Psi = U \Psi', \quad \bar{\Psi} = \bar{\Psi}' U^\dagger \quad (69)$$

with

$$U = \frac{1}{\sqrt{2t}} \begin{pmatrix} 0 & -i & 1 & 0 \\ i & 0 & 0 & 1 \\ 0 & -i & -1 & 0 \\ i & 0 & 0 & -1 \end{pmatrix}, \quad (70)$$

and allowing the fluctuation of the gauge field, we obtain the canonical Dirac Lagrangian,

$$\mathcal{L} = \bar{\Psi}' \left[i\gamma_\mu (\partial_\mu - ia_\mu) + \frac{1}{t} \right] \Psi' + \frac{1}{g^2} f_{\mu\nu}^2, \quad (71)$$

where

$$\gamma_\mu = \begin{pmatrix} -\sigma_\mu & 0 \\ 0 & \sigma_\mu \end{pmatrix} \quad (72)$$

with the Pauli matrices σ_μ for $\mu = 1, 2, 3$. This is the 4-component Dirac fermion with mass $\frac{1}{t}$. Note that we obtained 4-component Dirac fermion even though the minimal Dirac fermion has two component in (2+1)-dimension[26]. This is because of the parity symmetry in our theory. A mass term involving only the 2-component Dirac fermion would have broken parity symmetry[27].

In (2+1) dimension only confinement phase can occur for the compact U(1) gauge theory with the massive Dirac fermions. Higgs phase can not occur because of the fermionic statistics of the fractional particle. In the exciton language this implies that the off-diagonal exciton can not condense with the coupling constants $\tilde{K}_n > 0$. This is consistent with the earlier observation that the low energy conditions (51) cannot be satisfied simultaneously for any choice of exciton phase. This is the result of the frustration. The frustration in the interaction is closely related to the fermionic nature of fractionalized particle. And the spin follows the fermionic statistics. In this sense both the emergent fermionic statistics and the spin are the results of the frustration in the bosonic matrix model. In (3+1)-dimension the confinement to deconfinement phase transition can occur. For small t , the confining phase arises where the fractional fermions are confined by the U(1) gauge field. For large t , the massless U(1) gauge field (photon) and gapped fermions emerges as low energy excitations. The schematic phase diagram in (3+1)-dimension is shown in Fig. 3 (b).

It must be emphasized that the fractionalized fermion is a different object from the original fermion of the microscopic Hamiltonian (1). The original fermion is spinless and has no internal gauge charge, but it carries electromagnetic (EM) charge. The fractionalized fermion has spin and charge for the internal gauge field. The only quantum number they have in common is the flavor index. Moreover the fractionalized fermion is particle-hole symmetric, while the original fermions are in general not in that $m^c \neq m^d$.

IV. DUALITY MAPPING OF THE COMPACT U(1) GAUGE THEORIES WITH MASSIVE MATTER FIELDS

In the next section, we will describe the matrix models in dual representation. The goal of the dual description is to provide a more vivid picture of fractionalization and the emergent gauge field by describing the same phenomena in terms of the original exciton language. Before

doing that, in this section we will review the dual representation of the compact U(1) gauge theory coupled with matter fields. This will help to identify what plays the role of the fractionalized particle and the gauge field in the original exciton picture which will be discussed in the next section.

A. bosonic matter

In this section we discuss the dual representation of the compact U(1) gauge theory coupled with bosonic matter field. The action (32) is rewritten

$$S = -\frac{t}{2} \sum_i \sum_\mu (\cos(\phi(i+\mu) - \phi(i) - a_\mu(i)) - 1) - \sum_C \frac{1}{2g_C^2} (\cos b_C - 1). \quad (73)$$

Here i is lattice site and μ refers to D positive direction of link. t is the phase stiffness of boson and g_C , the generalized gauge coupling associated with the flux through a loop C . Each loop is assigned a unique orientation and $b_C = \oint_C a$. The choice of orientation does not matter because of the $\cos(b_C)$. The summation of C in the second term in Eq. (73) is over all possible closed loops. If only the smallest plaquette is allowed for the gauge kinetic term, Eq. (73) reduces to the well known Abelian-Higgs model[28]. Using the Villain approximation, we write the partition function,

$$Z = \int Da \int D\phi \sum_{p_\mu(i)=-\infty}^{\infty} \sum_{q_C=-\infty}^{\infty} \exp\left(-\frac{t}{4} \sum_{i,\mu} \{\phi(i+\mu) - \phi(i) - a_\mu(i) - 2\pi p_\mu(i)\}^2 - \sum_C \frac{1}{4g_C^2} \{b_C - 2\pi q_C\}^2\right). \quad (74)$$

Hubbard-Stratonovich transformation for the quadratic terms leads to

$$Z = \int Da \int D\phi \int D l_\mu \int D n_C \sum_{p_\mu(i), q_C} \exp\left(-\frac{1}{t} \sum_{i,\mu} (l_\mu(i))^2 - i \sum_{i,\mu} l_\mu(i) \{\phi(i+\mu) - \phi(i) - a_\mu(i) - 2\pi p_\mu(i)\} - \sum_C g_C^2 n_C^2 - i \sum_C n_C \{b_C - 2\pi q_C\}\right). \quad (75)$$

From the identity $\sum_{n=-\infty}^{\infty} e^{2\pi i n x} = \sum_{n=-\infty}^{\infty} \delta(x - n)$ the partition function becomes the sum over integer fields,

$$Z = \int Da \int D\phi \sum_{l_\mu(i), n_C} \exp\left(-\frac{1}{t} \sum_{i,\mu} (l_\mu(i))^2\right)$$

$$\begin{aligned}
& -i \sum_{i,\mu} l_\mu(i) \{ \phi(i+\mu) - \phi(i) - a_\mu(i) \} \\
& - \sum_C g_C^2 n_C^2 - i \sum_C n_C b_C \}. \quad (76)
\end{aligned}$$

Integrating out ϕ and a we obtain the constraint for the current conservation of boson and the flux conservation of the electric flux line,

$$\begin{aligned}
Z = & \sum_{l_\mu(i), n_C} \exp \left(-\frac{1}{t} \sum_{i,\mu} (l_\mu(i))^2 - \sum_C g_C^2 n_C^2 \right) \times \\
& \left(\prod_i \delta_{\sum_\mu \Delta_\mu l_\mu(i), 0} \right) \left(\prod_{i,\mu} \delta_{l_\mu(i) - \sum_{C' \ni (i,\mu)} S(C', i, \mu) n_{C'}, 0} \right). \quad (77)
\end{aligned}$$

Here $l_\mu(i)$ is integer defined on link. Nonzero value of it at a given line (i, μ) represents that the link is a part of world lines of boson(s). Negative value represents world line of anti-boson. The first constraint in the second line of (77) implies that the world line of boson should form closed loop. This is the result of current conservation of boson. n_C is an integer valued ‘field’ assigned to the loop C , i.e., it is defined on the space of loops, the set of all possible closed loops. The typical size of the loop is given by the inverse mass of the integrated matter field. It is convenient to think of the loop as a boundary of a surface. Then nonzero value of n_C implies that the surface enclosed by C is a part of a world sheet passing through the surface. The value with $n_C > 1$ is regarded as multiple world sheets and negative value, a world sheet of opposite orientation. The sign $S(C, i, \mu)$ which appears in the second constraint in Eq. (77) is 1 (−1) if the orientation of C is along (against) the vector μ associated with the (i, μ) . This constraint implies that such world sheet cannot end by itself. In the absence of boson current ($l_\mu(i) = 0$) the end of one world sheet should be joined by the end of another world sheet of same orientation. This means that they should form oriented closed surface in space-time. In the presence of boson current ($l_\mu(i) \neq 0$) the world sheet can end on the world line of boson. In lattice gauge theory, $n_C \neq 0$ represents the presence of quantized electric flux on that link. Thus the bosons serve as sources of the electric flux lines. The second constraint in Eq. (77) is the flux conservation law. Note that the world sheet is not well-defined in the lattice scale because of the uncertainty in determining a unique surface enclosed by a loop. We can define a smoothly varying surface only in the long distance scale larger than the typical length of the loops. This is attributed to the fact that gauge theory emerges only in the energy scale lower than the mass of the integrated matter field.

B. fermionic matter

Here we consider the compact U(1) gauge theory coupled with fermion in (65),

$$\begin{aligned}
S = & -t \sum_i \sum_{\pm\mu} e^{ia_\mu(i)} \psi_{i+\mu}^* \psi_i \\
& + \sum_i \psi_i^* \psi_i - \sum_C \frac{1}{2g_C^2} (-\cos b_C - 1). \quad (78)
\end{aligned}$$

Here $\pm\mu$ denote the nearest neighbor link in all $2D$ directions and $a_{-\mu}(i+\mu) = -a_\mu(i)$. Note that the sign of the gauge kinetic energy term is opposite to that of (73). We introduce an additional phase π in the flux term to apply the usual Villain approximation and the Hubbard-Stratonovich transformation,

$$e^{\frac{1}{2g_C^2} (-\cos b_C - 1)} = \sum_{n_C} e^{-\sum_C g_C^2 n_C^2 - i \sum_C n_C (b_C - \pi)}. \quad (79)$$

For the matter field we expand in t ,

$$\begin{aligned}
Z_\psi & \equiv \int D\psi^* D\psi e^{t \sum_i \sum_{\pm\mu} e^{ia_\mu(i)} \psi_{i+\mu}^* \psi_i - \sum_i \psi_i^* \psi_i} \\
& = \sum_{n=0}^{\infty} \frac{1}{n!} \left\langle \left(t \sum_i \sum_{\pm\mu} e^{ia_\mu(i)} \psi_{i+\mu}^* \psi_i \right)^n \right\rangle, \quad (80)
\end{aligned}$$

where $\langle A \rangle \equiv \int D\psi^* D\psi A e^{-\sum_i \psi_i^* \psi_i}$. Because of the conservation of matter current, only loop of fermion world lines contribute to the partition function,

$$Z_\psi = \sum_{m=0}^{\infty} (-1)^m \sum_{C_1, \dots, C_m} t^{\sum_{l=1}^m L(C_m)} e^{i \sum_{l=1}^m \oint_{C_l} a}. \quad (81)$$

Here m is the number of fermion loops where each loop is represented as C_m . There is a distinction of orientation for each fermion loop which is determined by the direction of fermion current. Unlike the bosonic case there is no ambiguity in counting the number of loops. This is because two loops cannot intersect owing to the anti-commutativity $\psi_i^2 = 0$. $L(C_m)$ is the length of each loop and $\oint_{C_l} a$ is the U(1) gauge flux penetrating the loop. The alternating sign with the number of fermion loops originates from the anticommutativity of the Grassmann field. Using (79) and (81) and integrating out the gauge field we obtain

$$\begin{aligned}
Z = & \sum_{l_\mu(i)=0, \pm 1} \sum_{n_C} (-1)^{m(l_\mu)} e^{-\sum_C (g_C^2 n_C^2 - i\pi n_C)} t^{\sum_{(i,\mu)} |l_\mu(i)|} \\
& \times \left(\prod_i \delta_{\sum_\mu \Delta_\mu l_\mu(i), 0} \right) \left(\prod_{i,\mu} \delta_{l_\mu(i) - \sum_{C' \ni (i,\mu)} S(C', i, \mu) n_{C'}, 0} \right). \quad (82)
\end{aligned}$$

Here $m(l_\mu)$ is the number of fermion loops for a given configuration of $l_\mu(i)$. This is similar to the action with the bosonic matter in (77) except that $l_\mu(i)$ can have only 0 and ± 1 , $e^{-1/t}$ is replaced with t and there is a factor (-1) for each fermion loop and n_C . The minus sign for each n_C originates from the opposite sign in the gauge kinetic energy term.

V. DUAL APPROACH TO THE EMERGENT U(1) GAUGE THEORY IN THE MATRIX MODELS

In this section we dualize the three different theories of (19) in the world line representation of exciton. The frac-

tionalization, the emergence of photon in the Coulomb phase and the statistics of the fractionalized particle will be discussed in the exciton language.

A. Duality description of fractionalized boson and U(1) gauge field

Consider the effective action for off-diagonal phases of the Hermitian matrix with $\tilde{K}_n < 0$,

$$S = -\frac{\kappa}{2} \sum_i \sum_\mu \sum_{a < b} [\cos(\theta^{ab}(i + \mu) - \theta^{ab}(i)) - 1] - \sum_{n=3}^{\infty} \frac{\kappa_n}{2} \sum_i \sum_{[a_1, a_2, \dots, a_n]} \left[f^{[a_1, a_2, \dots, a_n]} \cos\left(\sum_{l=1}^n \theta^{a_l a_{l+1}}(i)\right) - 1 \right]. \quad (83)$$

Here $\theta^{ab} = -\theta^{ba}$ is the phase of the Hermitian matrix. We defined $a_{n+1} \equiv a_1$ for notational simplicity. $\kappa = 2K\chi_o^2$ and $\kappa_n = 4n|\tilde{K}_n|\chi_o^n$. The summation $[a_1, a_2, \dots, a_n]$ is over all a_1, \dots, a_n modulo cyclic permutation and the reverse of the order of indices. No repeated consecutive indices are allowed, that is, $a_i \neq a_{i+1}$. $f^{[a_1, a_2, \dots, a_n]}$ is a symmetry factor which compensates the double counting in the cyclic permutation and the reverse of the indices. For example, $f^{[1, 2, 3]} = f^{[1, 2, 3, 4]} = 1$ and $f^{[1, 2, 3, 1, 2, 3]} = \frac{1}{2}$, etc. With the Villain approximation for both the kinetic energy term and the interaction term, the partition function becomes

$$Z = \int D\theta \sum_{p_\mu^{ab}(i)=-\infty}^{\infty} \prod_{n=3}^{\infty} \left(\sum_{q_{[a_1, \dots, a_n]}(i)=-\infty}^{\infty} \right) \exp\left[-\frac{\kappa}{4} \sum_{i, \mu, a < b} \{\theta^{ab}(i + \mu) - \theta^{ab}(i) - 2\pi p_\mu^{ab}(i)\}^2\right] - \sum_{n=3}^{\infty} \frac{\kappa_n}{4} \sum_i \sum_{[a_1, a_2, \dots, a_n]} f^{[a_1, a_2, \dots, a_n]} \left\{ \sum_{l=1}^n \theta^{a_l a_{l+1}}(i) - 2\pi q_{[a_1, \dots, a_n]}(i) \right\}^2. \quad (84)$$

Introducing two Hubbard-Stratonovich fields $l_\mu^{ab}(i)$ and $V^{[a_1 \dots a_n]}(i)$ and performing the summation over $p_\mu^{ab}(i)$ and $q_{[a_1, \dots, a_n]}(i)$, the partition function becomes sum over integer numbers for the exciton current and interaction vertex,

$$Z = \sum_{l_\mu^{ab}(i), V^{[a_1 \dots a_n]}(i)} \exp\left(-\frac{1}{\kappa} \sum_{i, \mu, a < b} (l_\mu^{ab}(i))^2 - \sum_{n=3}^{\infty} \sum_i \sum_{[a_1, a_2, \dots, a_n]} \frac{1}{\kappa^{[a_1 \dots a_n]}} (V^{[a_1 \dots a_n]}(i))^2\right) \times \int D\theta \exp\left(-i \sum_{i, \mu, a < b} l_\mu^{ab}(i) \{\theta^{ab}(i + \mu) - \theta^{ab}(i)\} - i \sum_{n=3}^{\infty} \sum_i \sum_{[a_1, a_2, \dots, a_n]} V^{[a_1 \dots a_n]}(i) \sum_{l=1}^n \theta^{a_l a_{l+1}}(i)\right), \quad (85)$$

where $\kappa^{[a_1 \dots a_{2n}]} = \kappa_{2n} f^{[a_1, a_2, \dots, a_{2n}]}$. Here $l_\mu^{ab}(i)$ represents current of ab excitons and $V^{[a_1 \dots a_n]}(i)$, vertex of interaction. The free energy cost of unit current in a link is $\frac{1}{\kappa}$ and that of unit vertex at a site is $\frac{1}{\kappa^{[a_1 \dots a_n]}}$. Integration over the exciton phase leads to current conservation

condition,

$$\sum_\mu \Delta_\mu l_\mu^{ab}(i) - \sum_n \sum_{a_3, \dots, a_n} (V^{[aba_3 \dots a_n]} - V^{[baa_3 \dots a_n]}) = 0. \quad (86)$$

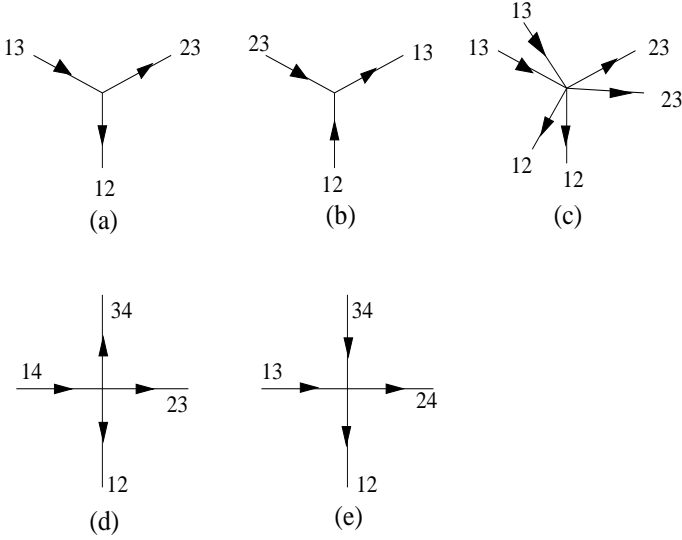


FIG. 4: Examples of vertices in the world line representation of exciton with (a) $V^{123} = 1$, (b) $V^{213} = 1$, (c) $V^{123} = 2$, (d) $V^{1234} = 1$ and (e) $V^{1243} = 1$. An incoming ab -exciton is same as an outgoing ba -exciton because χ is Hermitian. The direction of the exciton world line attached to vertices are drawn with the reference of ab -exciton with $a < b$.

The constraint (86) implies that the vertex $V^{[a_1 a_2 \dots a_n]}$ is a source or sink of the currents. Exciton current of each flavor is conserved if $V^{[a_1 a_2 \dots a_n]} = 0$ for all $[a_1 a_2 \dots a_n]$. If $V^{[a_1 a_2 \dots a_n]}(i) \neq 0$, the site i becomes a source for currents $j^{a_1 a_2}, \dots, j^{a_i a_{i+1}}, \dots, j^{a_n a_1}$ and a sink for the currents $j^{a_2 a_1}, \dots, j^{a_{i+1} a_i}, \dots, j^{a_1 a_n}$. Examples of the vertices are shown in Fig. 4(a)-(e). The vertices describe interaction among excitons. One species of exciton is annihilated and other exciton is created at the vertex as constituent fermion exchange their partners. Even though the exciton current of each species is not conserved at vertex, the flavor current is always conserved. This becomes more transparent if we represent exciton world line in double lines (see Fig. 5).

In the double line representation the link with $l_\mu^{ab}(i) = 1$ can be viewed as two world lines of a particle of flavor a and an anti-particle of flavor b . Each single line will be interpreted as the world line of the emergent fractional boson. Since each flavor current is always conserved, the single line should form loop. The single line should represent the world line of boson not fermion because the phase factor associated with the loop of single line is 1. This is consistent with the earlier discussion in Sec. III. A. At this stage the boson is just a ‘book-keeping’ tool for the exciton flavor. Whether this boson occurs as a low energy excitation or not is a dynamical question. In the weak coupling limit ($\kappa_n \ll 1$) the energy cost of a vertex is very high. Each exciton maintains its identity and the boson is confined within a single exciton for a long time $1/\kappa_n$. The low energy physics is described by weakly interacting excitons. This is the disordered phase of the off diagonal exciton condensate. It is in the strong

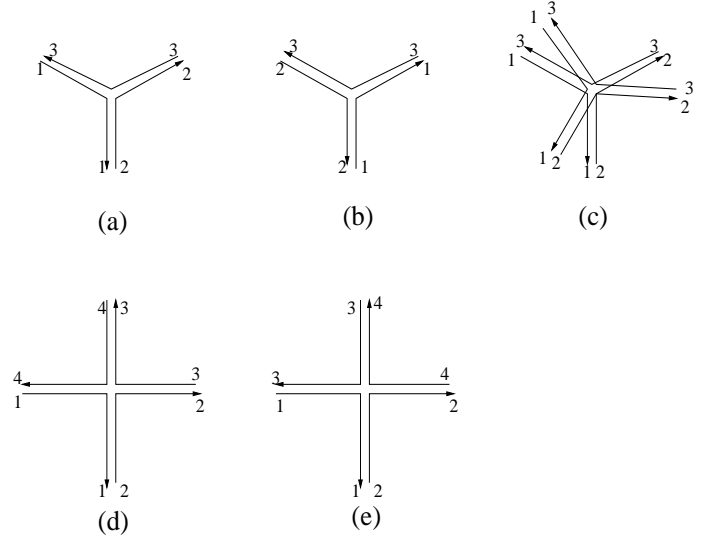


FIG. 5: Double line representation of the same vertices shown in Fig. 4 with (a) $V^{123} = 1$, (b) $V^{213} = 1$, (c) $V^{123} = 2$, (d) $V^{1234} = 1$ and (e) $V^{1243} = 1$. The world line of exciton with flavor ab is denoted as two lines where one line of flavor a moves in the same direction as the exciton world line and the other line of flavor b in the opposite direction.

coupling limit ($\kappa_n \gg 1$) where the bosons have chance to be liberated. In the strong coupling limit the vertex is cheap and exciton completely loses its identity within the discretized time (distance) scale. The scattering occurs so often that the boson is no longer confined within a single exciton. The exciton is not a quasiparticle. On the other hand the fractional boson can propagate for much longer time (distance) than exciton as they keep changing their partner. Then the fractional boson emerges as low energy excitation of the system. Some remarks are in order for the fractionalization. First, it does not mean that an exciton is really separated into two fractional bosons. Instead a boson is always part of some exciton. The point is that a boson is liberated from a particular exciton by frequently changing its partner in the strong coupling limit. Then the boson (anti-boson) appears to be free in the medium of other anti-bosons (bosons). (However the boson is not necessarily a quasiparticle because of the coupling to an emergent photon as will be discussed below.) It is emphasized again that the drastic change from the exciton quasiparticle picture to the fractionalization is due to the strong interaction. Second, the concept of fractionalization can be useful in an intermediate energy scale even in the case where there is no fractionalization in the low energy limit. In the following we explain these in more detail.

First we consider what configurations contribute to partition function (85). The world line of the fractional boson forms closed loop and is accompanied with another line with opposite current. The simplest configuration is two overlapped loops with current of flavor a in one direction and b in the other direction. It describes a pro-

cess where ab -exciton and ba -exciton pop out of vacuum and annihilate. In this sense the ab and ba -excitons are anti-particles to each other even though they are two independent excitons. This is a consequence of the condensation of diagonal excitons. Two diagonal excitons (aa and bb) in condensate collide to become two off-diagonal excitons (ab and ba) vice versa. The role of the phase coherent diagonal excitons is important even though it is hidden behind the dynamical stage. Note that we have $\theta^{ab} = -\theta^{ba}$ because of the mass term in (16) which is generated by the phase coherent diagonal excitons. General configurations consist of a collection of connected webs made of boson world lines (world line web). Each world line web defines closed surfaces as depicted in Fig. 6. Many such closed surfaces may co-exist and interpenetrate each other. It is noted that the closed surfaces made of the world line web are oriented. This is because the boson current has direction and only two currents with opposite direction can share a link. However, can we still define the orientation even if there is a crossing of flavor in a vertex? The answer is yes. One crossing diagram is shown in Fig. 7 (a). The crossing vertex in Fig. 7 (a) can be obtained from the non-crossing vertex in Fig. 7 (b) through a continuous deformation involving rotation as is shown in the figure. The oriented nature of the surface has important consequences for the gauge group of the emergent gauge field and the statistics of the fractional particle as will be shown below. Note that there are three independent length scales in the world line web. The shortest scale is the length of double line segment (ξ_1) which corresponds to the life time of a single exciton. The other is the size of the loop of single line (ξ_2) which is the life time of the fractional boson. Note that there is distribution in the size of the loops of single lines from the small loop of size ξ_1 to the large loop whose size is much larger than ξ_1 . The smaller loops of size ξ_1 are filling the area between the large loops of size ξ_2 . Even though there exist large loops of single lines, the life time of a single exciton is kept to be ξ_1 . This is how the fractional boson can emerge as low energy excitations. The largest length scale is the size of the bubble made of the web (ξ_3). In general we have $\xi_1 < \xi_2 < \xi_3$. In the following the confinement, Coulomb and Higgs phases are described in terms of the dynamics of the web.

In the small κ limit, all length scales are of order of lattice scale. As κ increases ξ_2 and ξ_3 increases. However ξ_1 remains almost same for fixed coupling constants ($\kappa_n \gg 1$). For $\xi_2 \ll \xi_3$ the closed surface of the world line web is well-defined in the length scale $x \sim \xi_3$. Thus the low energy theory reduces to the statistical problem of fluctuating surface. The surface can be regarded as the world sheet of oriented closed string. The string tension is determined by the density of exciton and κ . In the gauge theory picture the string corresponds to electric flux line and the string tension, the gauge coupling. The gauge group should be $U(1)$. This comes from the orientedness of the surface. In contrast, in the Z_n gauge theory there are lines where n currents of same direction

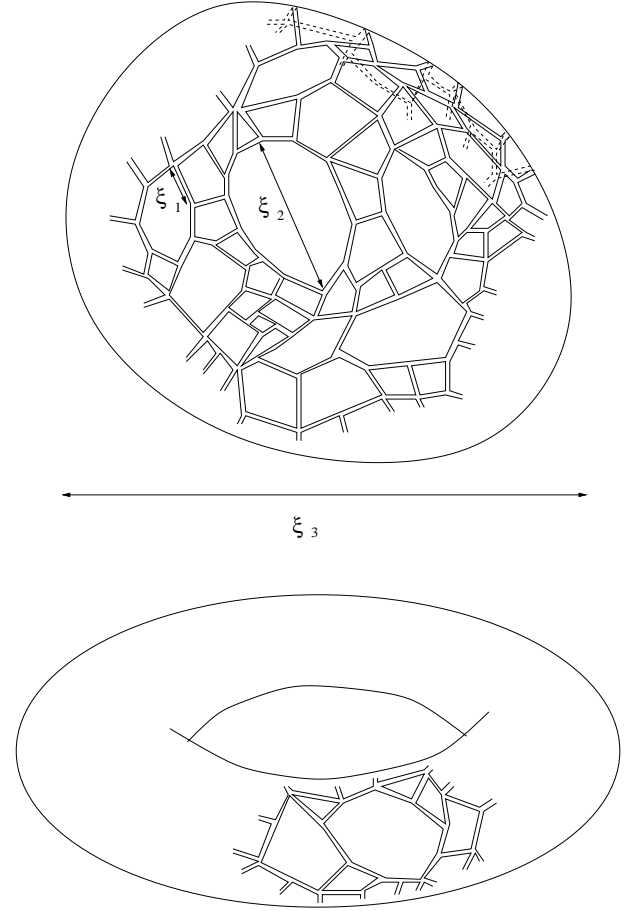


FIG. 6: Sphere and torus formed by web of exciton world lines.

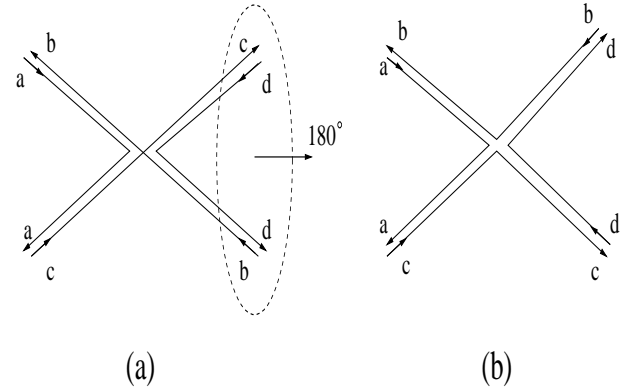


FIG. 7: Crossing vertex as a twisted uncrossed vertex.

can meet. Then n surfaces can join at these lines. This leads to an unoriented surface. If ξ_3 is finite there is finite tension for the world sheet of electric flux line. ξ_3 corresponds the confining scale. How can we probe the confining gauge field? This can be done by examining the potential energy between the two fractional bosons.

Consider creating two excitons of flavors ab and bc separated by distance r . Then ask the probability amplitude

for the two excitons to end up with excitons of flavors $\bar{a}d$ and $\bar{d}c$ after $\tau = \tau_1$. We follow only the flavor of a and c

by tracing out flavor b and d and measure

$$V(r) \equiv - \lim_{\tau_1 \rightarrow \infty} \frac{1}{\tau_1} \ln \sum_{b,d} \left\langle e^{-i(\theta^{ad}(\mathbf{i}, \tau_1) + \theta^{dc}(\mathbf{i}+\mathbf{r}, \tau_1))} e^{i(\theta^{ab}(\mathbf{i}, 0) + \theta^{bc}(\mathbf{i}+\mathbf{r}, 0))} \right\rangle, \quad (87)$$

where \mathbf{i} and \mathbf{r} is the (D-1)-dimensional space vector and τ , the imaginary time. The world line of the b and d bosons will be present only for a finite time scale near $\tau = 0$ and τ_1 respectively. After an initial transient time, we are left with boson a and anti-boson c connected by the world line web as is shown in Fig. 8. The end point of the web is the fractional boson and the web is the electric flux line connecting them. Thus we effectively measure the potential energy between the fractional bosons. If $\xi_2 \ll r \ll \xi_3$ two test bosons separated by r are subject to Coulomb interaction, $V(r) \sim \ln r$ for $D = 3$ and $V(r) \sim -1/r^{D-3}$ for $D > 3$. This is because the world line web fluctuates wildly in this length scale. The linear potential, $V(r) \sim r$, sets in for $\xi_3 \ll r \ll \frac{\xi_3^2}{\xi_2}$ where the electric flux line is almost straight. For $r \gg \frac{\xi_3^2}{\xi_2}$ the energy associated with the extended electric flux line exceeds the mass gap of fractional boson. The boson and anti-boson pop out to screen the test bosons and create two separate excitons. Then the potential becomes flat, $V(r) \sim \text{constant}$. This is what we observe in the confinement phase of the U(1) gauge theory with massive bosons. In the intermediate energy scale $1/\xi_3 \ll E \ll 1/\xi_2$ the effective theory is the emergent pure U(1) gauge field with almost gapless photon. It is known that pure compact U(1) gauge theory is always confined in 2+1 dimension. This means that ξ_3 is always finite and in the lowest energy scale $E \ll 1/\xi_3$ every excitation is gapped. The Coulomb phase is not a stable phase but can exist only as a cross-over. In space dimension greater than 2 the real Coulomb phase can arise even in the low energy limit. In the following we discuss the Coulomb phase.

As κ increases further, the bubbles grow and overlap. The surfaces of two bubble can re-connect to form a large and a small bubbles. In this way an infinitely large surface can form and the length scale ξ_3 diverges while ξ_2 remains finite. The world line web condenses (but not the individual boson). The low energy excitation is the collective excitation of the condensed world line web. In a given time slice, the intersection of the web surface with the time slice forms strings. In the deconfined phase, these strings are infinite in extent. This is a space-time picture for the string-net condensation[29]. In the gauge theory language the electric flux lines are the strings which are condensed, and the low energy collective excitation becomes the gapless ‘photon’. This is

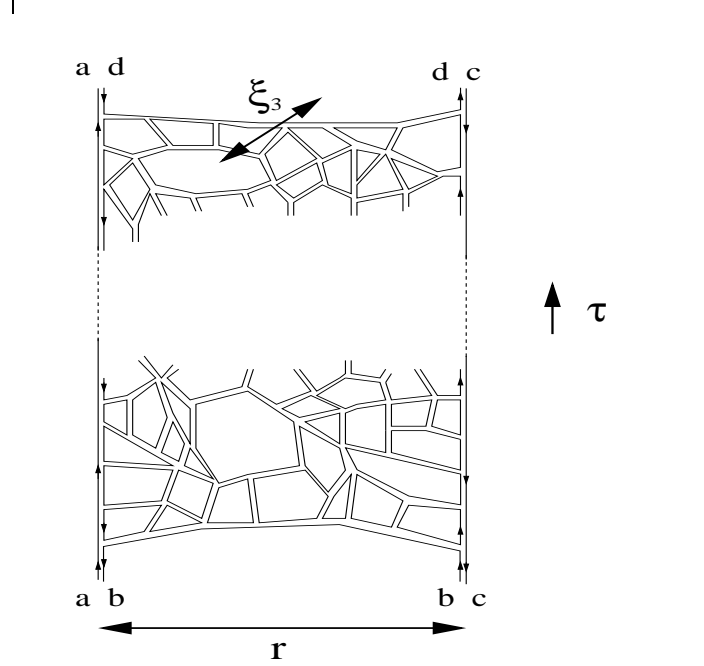


FIG. 8: Propagation of two excitons separated by distance r in the confinement phase. The end points of the web are boson and anti-boson, and the web is the electric flux line connecting them. ξ_3 is the length scale associated with the transverse fluctuations of the web.

the Coulomb (deconfinement) phase.

What is the massless ‘photon’ in terms of original exciton? To answer the question we first construct the Wilson operator. The Wilson operator creates a closed electric flux line in the gauge theory picture. Since the world sheet of electric flux line corresponds to world line web in the exciton picture, the Wilson operator corresponds to creation operator of series of excitons. However in order to create low energy excitations, the operator needs to create excitons in a special order along the loop, as we see from the following argument. The world line web corresponding to low energy excitations need to have large number of loops. This is because each loop contributes $-\ln N$ (N , the number of flavor) to the action. From this consideration we identify the Wilson operator,

$$W_{i_1 i_2 \dots i_n} \sim \sum_{a_1 a_2 \dots a_n} e^{i(\theta_{i_1}^{a_1 a_2} + \theta_{i_2}^{a_2 a_3} + \dots + \theta_{i_n}^{a_n a_1})}. \quad (88)$$

This operator creates a series of exciton along a contour C defined by the sites i_1, \dots, i_n . The neighboring excitons

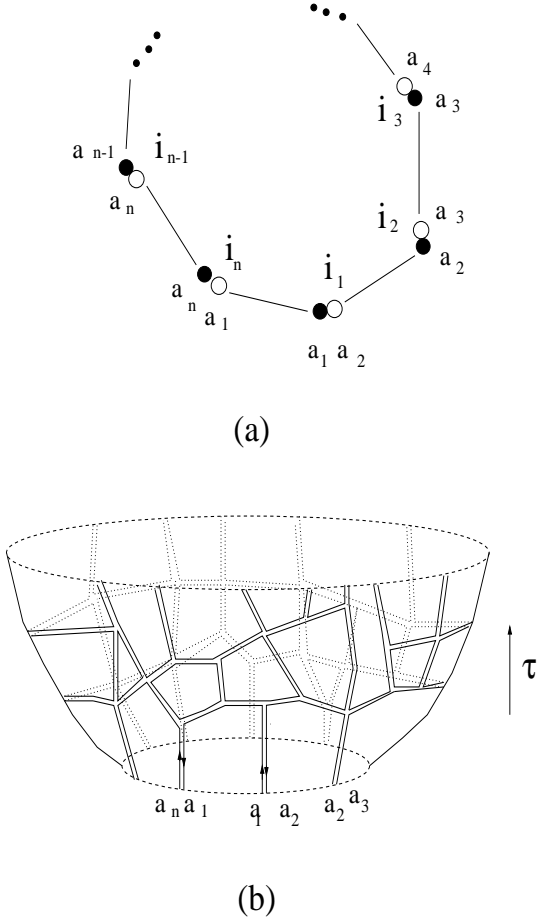


FIG. 9: (a) Series of excitons created by the Wilson operator. The solid (open) circle denotes flavor (anti-flavor) of exciton. (b) World sheet spanned by the time evolution of the Wilson operator.

have same flavor and anti-flavor (see Fig. 9 (a)). As the series of excitons propagate in time they can readily form a web as is shown in Fig. 9 (b). The correlation between flavors enables excitons to efficiently form a web maximizing the number of loops.

What does the Wilson operator do to existing excitons? It creates flavor current. For example if we apply $W \sim e^{i(\theta_i^{12} + \theta_j^{23} + \theta_j^{34} + \theta_i^{41})}$ to the states

$$\begin{aligned} |\Psi_1\rangle &= e^{i(\theta_i^{23} + \theta_j^{34} + \theta_j^{41} + \theta_i^{12})} |0\rangle, \\ |\Psi_2\rangle &= e^{i(\theta_i^{41} + \theta_j^{12} + \theta_j^{23} + \theta_i^{34})} |0\rangle \end{aligned} \quad (89)$$

with $|0\rangle$ being a vacuum without any off-diagonal exciton, we have

$$\begin{aligned} W|\Psi_1\rangle &= e^{i(\theta_i^{13} + \theta_j^{24} + \theta_j^{31} + \theta_i^{42})} |0\rangle, \\ W|\Psi_2\rangle &= e^{i(\theta_i^{42} + \theta_j^{13} + \theta_j^{24} + \theta_i^{31})} |0\rangle. \end{aligned} \quad (90)$$

Here we used the fact that once ab and bc excitons are on a site they decay into ac and bb excitons to lower energy by condensing the diagonal exciton. Keeping only the off-diagonal excitons we obtain the above result. This is

$$\begin{aligned} W_{ijkl} &= \begin{array}{c} \overline{1\ 2} \\ \begin{array}{|c|c|} \hline i & j \\ \hline \end{array} \\ \overline{2\ 3} \end{array} \begin{array}{c} \overline{4\ 1} \\ \begin{array}{|c|c|} \hline k & l \\ \hline \end{array} \\ \overline{3\ 4} \end{array} = \begin{array}{c} \overline{1\ 2} \\ \begin{array}{|c|c|} \hline i & j \\ \hline \end{array} \\ \overline{2\ 3} \end{array} \begin{array}{c} \overline{4\ 1} \\ \begin{array}{|c|c|} \hline k & l \\ \hline \end{array} \\ \overline{3\ 4} \end{array} \\ &= \begin{array}{c} \overline{1\ 1} \\ \begin{array}{|c|c|} \hline i & j \\ \hline \end{array} \\ \overline{2\ 2} \end{array} \begin{array}{c} \overline{4\ 4} \\ \begin{array}{|c|c|} \hline k & l \\ \hline \end{array} \\ \overline{3\ 3} \end{array} = \begin{array}{c} \overline{4\ 2} \\ \begin{array}{|c|c|} \hline i & j \\ \hline \end{array} \\ \overline{1\ 3} \end{array} \begin{array}{c} \overline{3\ 1} \\ \begin{array}{|c|c|} \hline k & l \\ \hline \end{array} \\ \overline{2\ 4} \end{array} \end{aligned} \quad (a)$$

$$\begin{aligned} W_{ijkl} &= \begin{array}{c} \overline{3\ 4} \\ \begin{array}{|c|c|} \hline i & j \\ \hline \end{array} \\ \overline{4\ 1} \end{array} \begin{array}{c} \overline{2\ 3} \\ \begin{array}{|c|c|} \hline k & l \\ \hline \end{array} \\ \overline{1\ 2} \end{array} = \begin{array}{c} \overline{3\ 4} \\ \begin{array}{|c|c|} \hline i & j \\ \hline \end{array} \\ \overline{4\ 1} \end{array} \begin{array}{c} \overline{2\ 3} \\ \begin{array}{|c|c|} \hline k & l \\ \hline \end{array} \\ \overline{1\ 2} \end{array} \\ &= \begin{array}{c} \overline{4\ 4} \\ \begin{array}{|c|c|} \hline i & j \\ \hline \end{array} \\ \overline{3\ 3} \end{array} \begin{array}{c} \overline{3\ 3} \\ \begin{array}{|c|c|} \hline k & l \\ \hline \end{array} \\ \overline{2\ 4} \end{array} = \begin{array}{c} \overline{3\ 1} \\ \begin{array}{|c|c|} \hline i & j \\ \hline \end{array} \\ \overline{4\ 2} \end{array} \begin{array}{c} \overline{2\ 4} \\ \begin{array}{|c|c|} \hline k & l \\ \hline \end{array} \\ \overline{1\ 3} \end{array} \end{aligned} \quad (b)$$

FIG. 10: The flavor current caused by the Wilson operator. ab indicates an exciton made of particle in the a -th band and hole in the b -th band. The Wilson operator induces the motion of boson in the counter-clockwise direction and anti-boson in the clockwise direction.

shown in Fig. 10. The Wilson operator induces flavor current in one direction (Fig. 10 (a)), and anti-flavor current (Fig. 10 (b)) in the other direction, thus inducing net flavor current. W_C^\dagger induces the opposite current and the rotational component of the flavor current can be identified as

$$\oint_C j_\mu^f dx^\mu \sim (W_C - W_C^\dagger), \quad (91)$$

where j^f is the flavor current.

With the excitonic expression for the Wilson operator we are readily to discuss the physical origin of the emergent photon. In the Coulomb phase there exist infinitely large bubbles of world line web. This causes long range correlation between the Wilson loop. Consider the correlator between the fluctuations of two Wilson loops,

$$\langle \delta W_{C_2}^\dagger \delta W_{C_1} \rangle, \quad (92)$$

where $\delta W_C = W_C - \langle W_C \rangle$ and C_1, C_2 are two loops separated by $\tau \gg \xi_2$ in the imaginary time direction.

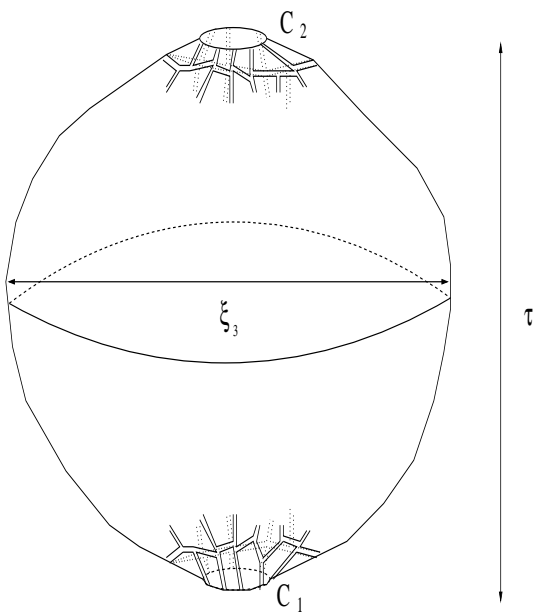


FIG. 11: The connected diagram contributing to the correlation function between two Wilson operators.

Since W_{C_1} ($W_{C_2}^\dagger$) creates (annihilates) world line web, the loops C_1 and C_2 becomes the boundary of the closed surface as is shown in Fig. 11. Only the connected diagram contribute to the correlator because the background value is subtracted. In the confining phase with finite ξ_3 , the contribution of the connected diagram is exponentially small for $\tau \gg \xi_3$. In the deconfinement phase, there are bubbles of arbitrarily large size which connect the C_1 and C_2 . This will leads to power law decay in the correlator, which signifies the presence of massless mode. This is the emergent photon in the Coulomb phase. In this way the emergent photon can be understood in terms of the exciton language. In the fractionalized boson picture, the emergent photon is the long-wavelength fluctuation of the flavor currents. The flavor current in Fig. 10 can be regarded as if the bosons are really liberated from the anti-bosons. On the other hand what is really happening is the concerted motion of the neutral excitons and the exchange of flavors between excitons on a site. Therefore the emergent boson should be electromagnetically neutral.

As κ keep increasing ξ_2 grows further. As seen from Fig. 6, areas with large ξ_2 correspond to punctures of the bubble. In the length scale $x \leq \xi_2$ the individual loops bordering the punctures on the 2-dimensional surface begin to be noticeable. The surface is no longer closed surface. The individual bosons form the boundary of world sheets and appear as low energy excitations (not necessarily quasiparticle). In a given time slice, the boson and anti-boson are the end of strings formed by the intersection of the web surface and the time slice[29]. So the low energy theory becomes the non-compact $U(1)$ gauge theory coupled with gapped bosons. In the large κ limit not only ξ_3 but also ξ_2 diverges. The fractional

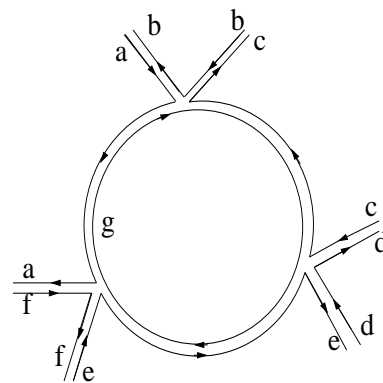


FIG. 12: The generation of the sixth order vertex from the quartic order vertices.

boson itself condenses. This is the Higgs phase. Unlike the Coulomb phase the Higgs phase can occur even in the 2+1 dimension.

B. Duality description of fractionalized boson, Ising mode and $U(1)$ gauge field

The duality mapping for the Hermitian matrix model with $\tilde{K}_{2n-1} = 0$ and $\tilde{K}_{2n} < 0$ is exactly same as the one in the previous section except for the fact that only vertices of even order are allowed. Thus we will not repeat the same procedure. Instead we will discuss the new feature which arises from the absence of vertex of odd order. As discussed in the Sec. III. B, there exists extra Z_2 degree of freedom which undergoes the disorder to order phase transition. How can we interpret the phase transition in the dual representation? We will show that the phase transition corresponds to a spontaneous generation of the odd order vertex. To see this, we first note that the presence of quartic vertex implies the presence of all higher vertices of even order. For example, Fig. 12 shows the generation of a sixth order vertex from the one-loop contribution. In the length scale larger than the loop, the sixth order vertex can be regarded as a local interaction. Two sixth order vertices can effectively act as two third order vertices connected by world lines of three excitons as is shown in Fig. 13. In the disordered phase of the Ising variable, the composite of the three excitons has only short range correlation. Thus the two third order vertices in Fig. 13 is linearly confined to each other. In the ordered phase the world line of the three excitons can be infinitely large. Thus the third order vertices are unbound. One can regard the \tilde{K}_3 term as an explicit symmetry breaking term for the Z_2 symmetry of the exciton Lagrangian. Then the generation of the third order vertex without bare \tilde{K}_3 is the spontaneous symmetry breaking of the Z_2 symmetry. In the world line picture it corresponds to the binding unbinding transition of the effective third order vertices made of the even order vertices.

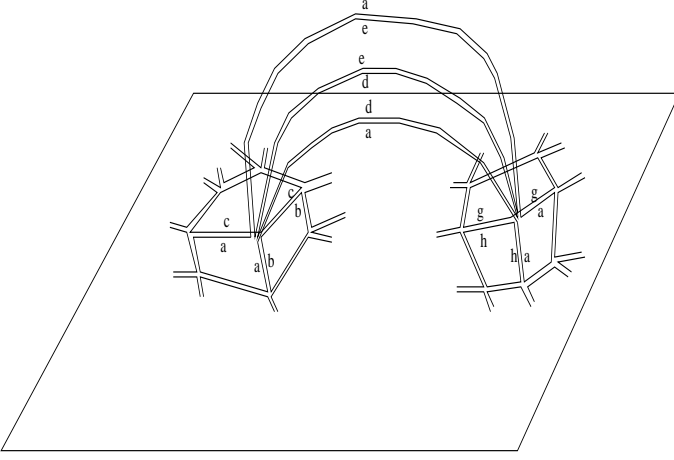


FIG. 13: Two sixth order vertices connected by the world lines of three excitons.

C. Duality description of fractionalized fermion, Ising mode and U(1) gauge field

Here we examine the anti-Hermitian matrix model with $\tilde{K}_{2n} > 0$. The duality mapping can be performed in a parallel way to the mapping for the fractionalized boson except for the two differences. First, the coefficients of the potential energy term has opposite sign. Second, the matrix is anti-Hermitian. These two differences cause the transmutation of the statistics of the fractional particle. The effective action for the off-diagonal phases is written

$$S = -\frac{\kappa}{2} \sum_i \sum_{\mu} \sum_{a < b} [\cos(\theta^{ab}(i + \mu) - \theta^{ab}(i)) - 1] - \sum_{n \geq 2} \frac{\kappa_{2n}}{2} \sum_i \sum_{[a_1, a_2, \dots, a_{2n}]} f^{[a_1, a_2, \dots, a_{2n}]} \left[\cos \left(\sum_{l=1}^{2n} \theta^{a_l a_{l+1}}(i) - \pi \right) - 1 \right], \quad (93)$$

where $\theta^{ab} = -\theta^{ba} + \pi$ is the phase of the anti-Hermitian matrix. Other notations are same as those in Sec. V. A. Note that there is an extra phase π in the potential term accounting for the opposite sign of the coupling constant.

From the Villain approximation and the Hubbard-Stratonovich transformations we obtain the similar partition function to (85),

$$Z = \sum_{l_{\mu}^{ab}(i), V^{[a_1 \dots a_{2n}]}(i)} Q_V \exp \left(-\frac{1}{\kappa} \sum_{i, \mu, a < b} (l_{\mu}^{ab}(i))^2 - \sum_{n=2}^{\infty} \sum_i \sum_{[a_1, a_2, \dots, a_{2n}]} \frac{1}{\kappa^{[a_1 \dots a_{2n}]}} (V^{[a_1 \dots a_{2n}]}(i))^2 \right) \times \int D\theta \exp \left(-i \sum_{i, \mu, a < b} l_{\mu}^{ab}(i) \{ \theta^{ab}(i + \mu) - \theta^{ab}(i) \} - i \sum_{n=2}^{\infty} \sum_i \sum_{[a_1, a_2, \dots, a_{2n}]} V^{[a_1 \dots a_{2n}]}(i) \sum_{l=1}^{2n} \theta^{a_l a_{l+1}}(i) \right). \quad (94)$$

The extra phase factor Q_V in the partition function is the consequence of the opposite sign in the coupling constant. It is given by

$$Q_V \equiv \exp \left(i\pi \sum_n \sum_i \sum_{[a_1, a_2, \dots, a_{2n}]} V^{[a_1 \dots a_{2n}]}(i) \right) \quad (95)$$

and it can be simply written as

$$Q_V = e^{i\pi V}, \quad (96)$$

where V is the total number of vertices in the polygon made of the exciton world lines. Besides Q_V , there is another phase arising from the anti-Hermiticity. Since θ^{ab} and θ^{ba} are not independent fields, one has to replace

θ^{ba} into $-\theta^{ab} + \pi$ for $a < b$ in integrating over θ^{ab} . After integration it leads to the same constraint as (86) but with another phase factor,

$$Q_E = \exp \left(-i\pi \sum_{n=2}^{\infty} \sum_i \sum_{[a_1, a_2, \dots, a_{2n}]} V^{[a_1 \dots a_{2n}]}(i) s^{[a_1 \dots a_{2n}]}(i) \right), \quad (97)$$

where

$$s^{[a_1 \dots a_{2n}]}(i) = \sum_{i=1}^{2n} \frac{1}{2} \left(\frac{a_i - a_{i+1}}{|a_i - a_{i+1}|} + 1 \right). \quad (98)$$

$s^{[a_1 \dots a_{2n}]}(i)$ counts the number of emanating exciton world lines attached to the vertex $V^{[a_1 \dots a_{2n}]}(i)$ whose

double index is in descending order (e.g. $s^{[1234]}(i) = 1$ because there is one descending double index 41 among 12, 23, 34, 41; similarly we have $s^{[1243]}(i) = 2$.) The second extra phase factor, in turn, becomes

$$Q_E = e^{-i\pi E}, \quad (99)$$

Finally we have

$$Z = \sum_{l_\mu^{ab}(i), V^{[a_1 \dots a_{2n}]}(i)} e^{i\pi(V-E)} \exp\left(-\frac{1}{\kappa} \sum_{i, \mu, a < b} (l_\mu^{ab}(i))^2 - \sum_{n=2}^{\infty} \sum_i \sum_{[a_1, a_2, \dots, a_{2n}]} \frac{1}{\kappa^{[a_1 \dots a_{2n}]}} (V^{[a_1 \dots a_{2n}]}(i))^2\right) \times \left(\prod_{i, a < b} \delta_{\sum_\mu \Delta_\mu l_\mu^{ab}(i) - \sum_n \sum_{a_3, \dots, a_{2n}} (V^{[aba_3 \dots a_{2n}]} - V^{[baa_3 \dots a_{2n}]}, 0)}\right). \quad (100)$$

The extra phase factor can be related to the number of faces F of the polygon because the Euler characteristic is a topological invariant,

$$\chi_{Euler} \equiv V - E + F = 2(1 - g), \quad (101)$$

where g is the genus of the surface. Since g is integer we have

$$e^{i\pi(V-E)} = e^{i\pi F}. \quad (102)$$

On the other hand the number of the faces is same as the number of the loops of single line. There is extra phase factor (-1) for every loop of single line. Thus each single line represents the world line of a fermion. For example the diagram in Fig. 15 (a) has 4 loops and Fig. 15 (b) has 5 loops of single line. They contribute to partition function with the opposite sign. This is the signature of the emergent fermion in the exciton partition function. As was mentioned before, the orientedness of the closed surface is important for the simple relation (102) because the Euler characteristic (101) can be odd integer for non-orientable surface. It is straightforward to obtain the same result from the Hermitian matrix model with $\tilde{K}_{2n} = (-1)^n |\tilde{K}_{2n}|$.

The confinement to deconfinement phase transition can be understood as the divergence of the scale of the world line web as discussed in Sec. V. A. The difference is that the bubbles made of exciton world lines contribute to the partition function with oscillating sign as the number of single line loops increases. The oscillating sign also appears in the partition function for the gauge theory coupled to fermions as seen from the phase factor $e^{i\pi n_C}$ in Eq. (82). Thus we see that this case corresponds to an emergent gauge theory with the opposite sign of the kinetic energy term (Eq. (78)).

The phase transition for the Z_2 variable can also be understood in the same way as discussed in Sec. V. B. The difference is that the ordered phase of the Ising variable is not related to the generation of the usual $\tilde{K}_3 \text{tr}' \chi^3$ term in (17). It cancels with its complex conjugate term

where E is the total number of exciton world line segments. This is because each exciton world line is attached to two vertices and the double index is in ascending order in one vertex and in descending order in the other vertex (see Fig. 14).

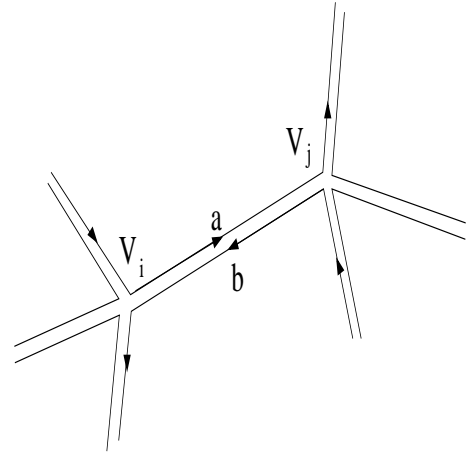


FIG. 14: ab -exciton is emanating from the vertex V_i and ba -exciton, from the vertex V_j . Thus there is one $e^{-i\pi}$ factor associated with the exciton world line either from V_i or V_j .

for the anti-Hermitian matrix. The spontaneously generated interaction in the ordered phase corresponds to a flavor dependent interaction,

$$\sum_{a \neq b \neq c} K_3^{abc} \chi^{ab} \chi^{bc} \chi^{ca} \quad (103)$$

with $K_3^{abc} = -K_3^{cba}$. With the flavor dependent coupling constant, the complex conjugate term no longer cancel each other under the anti-Hermitian constraint. Eq. (103) contributes to (93) as vertex of third order. Note that the overall sign of $K_3^{[a,b,c]}$ does not matter because the third order vertex should occur in pair because of the constraint between the number of vertices and the double line segments,

$$\sum_n n V_n = 2E. \quad (104)$$

Finally, the Higgs phase can not occur in this case because the fractional particle is fermion. In the world line

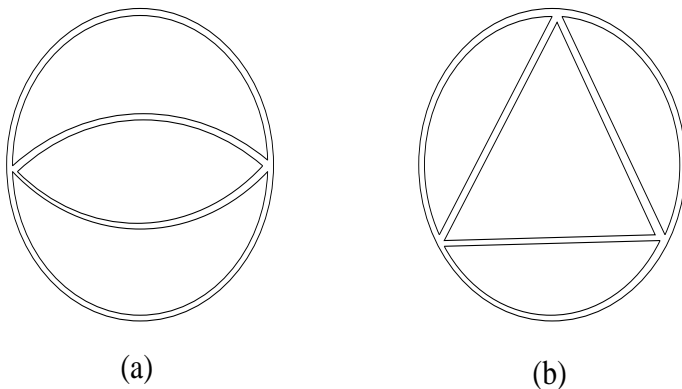


FIG. 15: Configurations of exciton world lines involving (a) 4 loops and (b) 5 loops of single line.

picture this may be related to the oscillating phase with the increasing number of the fractional fermion loops.

VI. CONCLUSIONS

In this paper we studied an exciton model which supports various fractionalized phases with either fractionalized boson or fermion along with emergent photon. Phenomenological matrix model for exciton bose condensate is derived from a microscopic theory. The statistics and spin of the fractionalized particles are determined dynamically. The bosonic fractionalized particle is shown to occur more generically. The fermionic nature of the fractionalized particle is shown to be rooted to frustration in the underlying bosonic matrix model. The fermionic statistics, in turn, is shown to be responsible for the generation of spin in the continuum limit in agreement with the spin-statistics theorem. The fractionalization is explained in two consistent point of views. One is based on more conventional approach where the fractionalized degrees of freedom are obtained from decomposition of original exciton field into multiple modes as required by constraints imposed by strong interaction. The other approach is based on the world line representation of original exciton. In the latter approach, a more vivid physical picture for the fractionalization is obtained in terms of the original exciton language, while more quantitative but abstract analysis is given in the first approach.

We close by making some comments on the observational consequences of the emergent photon and fractionalized particles in the Coulomb phase. The photon is the only gapless mode and will dominate the specific heat at low temperature, as T^3 in $d = 3$ and T^2 with cross-over to a small gap to $d = 2$. The fractionalization of the exciton will greatly affect the spectral properties. The exciton is not a well defined excitation. The exciton propagator is a product of two fractionalized particles in space-time, connected by a strongly fluctuating web, i.e. interacting via the exchange of photons. If the coupling to the photon is weak, it can be ignored and the exciton spec-

tral function is a convolution of two spectral functions of fractionalized particles, and will become extremely broad with an unusual line-shape.

VII. ACKNOWLEDGEMENTS

We thank X.-G. Wen and T. Senthil for illuminating discussions. This work was supported by the NSF grant DMR-0517222.

Appendix A. Effective action of exciton condensate and the saddle-point solutions

The objective of this appendix is two-folded. The first one is to derive the effective action (7)-(9) from the microscopic Hamiltonian (1). The second one is to present the saddle point solutions for the self-consistent equations for the exciton condensate field.

We rearrange the the attractive interaction as

$$\begin{aligned} & - \sum_{ab} V^{ab} \sum_{k,k',q} c_{k+q}^{a*} c_k^a d_{k'+q}^{b*} d_{k'}^b \\ & = - \sum_{ab} V^{ab} \sum_{k,k',q} d_k^{b*} c_{k+q}^a c_{k'+q}^{a*} d_{k'}^b, \end{aligned} \quad (\text{A1})$$

and introduce Hubbard-Stratonovich fields describing the exciton condensate to obtain

$$\begin{aligned} L_{int} & = \sum_{ab} \sum_q \left((V^{ab})^{-1} |\xi_q^{ab}|^2 - \frac{\xi_q^{ab}}{\sqrt{v}} \sum_{k'} c_{k'+q}^{a*} d_{k'}^b \right. \\ & \quad \left. - \frac{\xi_q^{ab*}}{\sqrt{v}} \sum_k d_k^{b*} c_{k+q}^a \right). \end{aligned} \quad (\text{A2})$$

With the anisotropic Coulomb interaction, $V^{ab} = V + V' \delta_{ab}$ and a dimensionless exciton field, $\chi^{ab} = \frac{\xi^{ab}}{V}$, the effective Lagrangian becomes

$$\begin{aligned} L & = V \sum_q \sum_{ab} |\chi_q^{ab}|^2 - \frac{VV'}{V+V'} \sum_q \sum_a |\chi_q^{aa}|^2 \\ & \quad + \sum_k \sum_a \left[c_k^{a*} (\partial_\tau + \epsilon_k^c - \mu) c_k^a + d_k^{a*} (\partial_\tau + \epsilon_k^d - \mu) d_k^a \right] \\ & \quad - \frac{V}{\sqrt{v}} \sum_q \sum_{ab} \left(\sum_k c_{k+q}^{a*} \chi_q^{ab} d_k^b + \sum_k d_k^{b*} \chi_q^{ab*} c_{k+q}^a \right) \\ & \quad + U \sum_k \sum_a (c_k^{a*} d_k^a + d_k^{a*} c_k^a). \end{aligned} \quad (\text{A3})$$

Absorbing the mixing (U) term into χ by a shift of the exciton field

$$\chi_q^{ab} = \chi_q'^{ab} + \frac{U}{V} \sqrt{v} \delta_{ab} \delta_{q,0}, \quad (\text{A4})$$

we finally obtain the Lagrangian,

$$\begin{aligned} L & = V \sum_q \sum_{ab} |\chi_q'^{ab}|^2 - \frac{VV'}{V+V'} \sum_q \sum_a |\chi_q'^{aa}|^2 \\ & \quad + \frac{VU}{V+V'} \sqrt{v} \sum_a (\chi_0'^{aa} + \chi_0'^{aa*}) \\ & \quad + \sum_k \sum_a \left[c_k^{a*} (\partial_\tau + \epsilon_k^c - \mu) c_k^a \right. \\ & \quad \left. + d_k^{a*} (\partial_\tau + \epsilon_k^d - \mu) d_k^a \right] \end{aligned}$$

$$\begin{aligned} & - \frac{V}{\sqrt{v}} \sum_q \sum_{ab} \left(\sum_k c_{k+q}^{a*} \chi_q'^{ab} d_k^b + \sum_k d_k^{b*} \chi_q'^{ab*} c_{k+q}^a \right) \\ & + \frac{NU^2}{V+V'} v \end{aligned} \quad (\text{A5})$$

From now on we omit the prime in the χ' and drop the last constant term.

Now we consider the mean-field solution for the exciton condensate. We consider a translationally invariant saddle point Ansatz,

$$\chi_q^{ab} = \sqrt{v} \chi^{ab} \delta_{q,0} \quad (\text{A6})$$

for the exciton condensate and solve the self-consistent equations for χ^{ab} ,

$$\left(1 - \frac{V'}{V+V'} \delta_{ab} \right) \chi^{ab} + \frac{U}{V+V'} \delta_{ab} = \frac{1}{v} \sum_k \langle d_k^{b\dagger} c_k^a \rangle. \quad (\text{A7})$$

Note that the saddle point equation for χ^{ab} has different form from (2) because of the rescaling and shift in χ^{ab} .

Here we present the saddle point solutions for $N = 3$ obtained in the 20×20 square lattice. For simplicity we use the particle-hole symmetric tight-binding dispersion, $\epsilon_k^c - \mu = -(\epsilon_k^d - \mu) = -t(\cos k_x + \cos k_y - 2) + \Delta$ with $t = 1$ and $\Delta = 1$. Various solutions are possible depending on the parameters of V, V', U . The followings are the saddle point solutions :

- $V = 10, V' = 5, U = 0$:

$$\chi^{ab} = \begin{pmatrix} \chi_d & 0 & 0 \\ 0 & \chi_d & 0 \\ 0 & 0 & \chi_d \end{pmatrix}, \quad (\text{A8})$$

with $\chi_d = 0.68$.

- $V = 10, V' = -5, U = 0$:

$$\chi^{ab} = \begin{pmatrix} 0 & \chi_1 & 0 \\ 0 & 0 & \chi_1 \\ \chi_1 & 0 & 0 \end{pmatrix}, \quad (\text{A9})$$

with $\chi = 0.4$.

- $V = 10, V' = -5, U = 0.3$:

$$\chi^{ab} = \begin{pmatrix} \chi_d & -\chi_1 & \chi_2 \\ -\chi_2 & \chi_d & -\chi_1 \\ \chi_1 & -\chi_2 & \chi_d \end{pmatrix}, \quad (\text{A10})$$

with $\chi_d = -0.06, \chi_1 = 0.07$ and $\chi_2 = 0.39$.

- $V = 10, V' = -5, U = 0.7$:

$$\chi^{ab} = \begin{pmatrix} \chi_d & \chi_o & \chi_o \\ \chi_o & \chi_d & \chi_o \\ \chi_o & \chi_o & \chi_d \end{pmatrix}, \quad (\text{A11})$$

with $\chi_d = -0.14$ and $\chi_o = 0.27$.

The above solutions are locally stable. However it is possible that they are not global minima. One may have to add further interaction term to stabilize the desired saddle point solution.

Appendix B. Derivation of Hermitian and anti-Hermitian matrix models

In this appendix we derive the Hermitian (17) and the anti-Hermitian matrix model (18) from the effective action of the exciton condensate (14). This is done by replacing the diagonal element of χ by the amplitude of the diagonal condensate, χ_d in (14) and extract the terms for the off-diagonal elements of χ . In the quartic interaction

$$K_4 \sum_{a,b,c,d} \chi_{ba}^* \chi_{bc} \chi_{dc}^* \chi_{da}, \quad (\text{B1})$$

there are 5 different possibilities of how the diagonal and off-diagonal elements are mixed depending whether 2, 1 or 0 of the χ fields are diagonal. This leads to the action for the off diagonal phase modes,

$$\begin{aligned} L_{K_4} &= K_4 \chi_d^2 tr'(\chi\chi + h.c.) \\ &\quad + 2K_4 \chi_d tr'(\chi\chi^\dagger\chi + h.c.) \\ &\quad + K_4 tr' \chi^\dagger \chi \chi^\dagger \chi, \end{aligned} \quad (\text{B2})$$

where $tr'(A_1 A_2 \dots A_n)$ denotes trace for the product of matrices which involves only the off-diagonal element of each matrix, e.g., $tr' AB = \sum_{a \neq b} A_{ab} B_{ba}$. Similarly, the sixth order interactions also give rise to potential energy for the off-diagonal phase modes,

$$\begin{aligned} L_{K_6} &= 3K_6 \chi_d^4 tr'(\chi\chi + h.c.) + K_6 \chi_d^3 tr'(\chi^3 + h.c.) \\ &\quad + 9K_6 \chi_d^3 tr'(\chi\chi^\dagger\chi + h.c.) + 3K_6 \chi_d^2 tr'(\chi^3 \chi^\dagger + h.c.) \\ &\quad + 3K_6 \chi_d^2 tr' \chi^\dagger \chi^\dagger \chi \chi + 6K_6 \chi_d^2 tr' \chi^\dagger \chi \chi^\dagger \chi \\ &\quad + 3K_6 \chi_d tr'(\chi\chi^\dagger \chi \chi^\dagger \chi + h.c.) \\ &\quad + K_6 tr' \chi \chi^\dagger \chi \chi^\dagger \chi \chi^\dagger, \\ L_{K'_6} &= NK'_6 (\chi_d^2 + (N-1)\chi_o^2) tr \chi^\dagger \chi \chi^\dagger \chi. \end{aligned} \quad (\text{B3})$$

$L_{K'_6}$ has the same form as L_{K_4} and this renormalizes K_4 into $K''_4 \equiv K_4 + NK'_6 (\chi_d^2 + (N-1)\chi_o^2)$. Summing L_{K_4} , L_{K_6} and $L_{K'_6}$ we have

$$L_K = (K''_4 \chi_d^2 + 3K_6 \chi_d^4) tr'(\chi\chi + h.c.)$$

$$\begin{aligned} &+ K_6 \chi_d^3 tr'(\chi^3 + h.c.) \\ &+ (2K''_4 \chi_d + 9K_6 \chi_d^3) tr'(\chi\chi^\dagger\chi + h.c.) \\ &+ 3K_6 \chi_d^2 tr'(\chi^3 \chi^\dagger + h.c.) \\ &+ 3K_6 \chi_d^2 tr' \chi^\dagger \chi^\dagger \chi \chi \\ &+ (K''_4 + 6K_6 \chi_d^2) tr' \chi^\dagger \chi \chi^\dagger \chi \\ &+ 3K_6 \chi_d tr'(\chi\chi^\dagger \chi \chi^\dagger \chi + h.c.) \\ &+ K_6 tr' \chi \chi^\dagger \chi \chi^\dagger \chi \chi^\dagger. \end{aligned} \quad (\text{B4})$$

For $\chi_o \ll 1$ the second order term of χ is most important. We rewrite the second order term in (B4),

$$\frac{\tilde{K}_2}{2} tr'(\chi\chi + h.c.) = \tilde{K}_2 tr' \chi_o^2 \sum_{a \neq b} \cos(\theta^{ab} + \theta^{ba}), \quad (\text{B5})$$

where

$$\begin{aligned} \tilde{K}_2 &\equiv 2(K''_4 \chi_d^2 + 3K_6 \chi_d^4) \\ &= 2\chi_d^2 [K_4 + NK'_6 (\chi_d^2 + (N-1)\chi_o^2) + 3K_6 \chi_d^2]. \end{aligned} \quad (\text{B6})$$

If $\tilde{K}_2 < 0$, the energy of (B5) is minimized by

$$\theta_i^{ab} = -\theta_i^{ba}. \quad (\text{B7})$$

This gives mass to the $\frac{N(N-1)}{2}$ symmetric modes with $\theta^{ab} = \theta^{ba}$. The remaining modes are $\frac{N(N-1)}{2}$ antisymmetric modes with $\theta^{ab} = -\theta^{ba}$. For $|\tilde{K}_2| \chi_o^2 \gg 1$, the symmetric modes are frozen and χ becomes Hermitian matrix ($\chi^\dagger = \chi$). If $\tilde{K}_2 > 0$, the energy of (B5) is minimized by

$$\theta_i^{ab} = -\theta_i^{ba} + \pi \quad (\text{B8})$$

and χ becomes anti-Hermitian matrix for $\tilde{K}_2 \chi_o^2 \gg 1$ ($\chi^\dagger = -\chi$). These Hermiticity or the anti-Hermiticity condition converts the dynamics of the off diagonal exciton into relativistic one. To see this we rewrite the first term in Eq. (13) as

$$\begin{aligned} S_\tau &= -\frac{K}{2} \sum_i tr' \chi_{i+\Delta\tau}^\dagger \chi_i \\ &= -\frac{K}{4} \sum_i tr' (\chi_{i+\Delta\tau}^\dagger \chi_i + \chi_{i+\Delta\tau} \chi_i^\dagger), \end{aligned} \quad (\text{B9})$$

where we used the Hermiticity or anti-Hermiticity condition in the last line. From this, we obtain the Hermitian matrix model,

$$S = -\frac{K}{4} \sum_{\langle i,j \rangle} tr' (\chi_i^\dagger \chi_j + h.c.) + \sum_{n \geq 3} \tilde{K}_n \sum_i tr' \chi_i^n, \quad (\text{B10})$$

with

$$\begin{aligned} \tilde{K}_3 &= 2[2K''_4 \chi_d + 10K_6 \chi_d^3], \\ \tilde{K}_4 &= K''_4 + 15K_6 \chi_d^2, \\ \tilde{K}_5 &= 6K_6 \chi_d, \\ \tilde{K}_6 &= K_6 \end{aligned} \quad (\text{B11})$$

for $\tilde{K}_2 < 0$, and the anti-Hermitian matrix model,

$$S = -\frac{K}{4} \sum_{\langle i,j \rangle} \text{tr}'(\chi_i^\dagger \chi_j + h.c.) + \sum_{n \geq 2} \tilde{K}_{2n} \sum_i \text{tr}' \chi_i^{2n}, \quad (\text{B12})$$

with

$$\begin{aligned} \tilde{K}_4 &= K_4'' + 3K_6 \chi_d^2, \\ \tilde{K}_6 &= -K_6 \end{aligned} \quad (\text{B13})$$

for $\tilde{K}_2 > 0$. Here $\langle i, j \rangle$ is the nearest neighbor in the D-dimensional (hyper) cubic lattice. χ is Hermitian (anti-Hermitian) matrix in Eq. (B10) ((B12)). Note that all odd order terms vanish in the anti-Hermitian matrix model because of the anti-Hermiticity, e.g.,

$$\text{tr}'(\chi^\dagger \chi \chi^\dagger + \chi \chi^\dagger \chi) = \text{tr}'(\chi^\dagger \chi \chi^\dagger - \chi^\dagger \chi \chi^\dagger) = 0. \quad (\text{B14})$$

-
- [1] F. D. M. Haldane, J. Phys. C. **14**, 2585 (1981).
[2] R. B. Laughlin, Phys. Rev. Lett. **50**, 1395 (1983).
[3] P. A. Lee, N. Nagaosa and X.-G. Wen, to appear in Rev. Mod. Phys. [cond-mat/0410445].
[4] P. W. Anderson, Science **235**, 1196 (1987); P. Fazekas and P. W. Anderson, Philos. Mag. **30**, 432 (1974).
[5] N. Read and S. Sachdev, Phys. Rev. Lett. **66**, 1773 (1991).
[6] X.-G. Wen, Phys. Rev. B **44**, 2664 (1991).
[7] T. Senthil and M. P. A. Fisher, Phys. Rev. B **62**, 7850 (2000).
[8] X.-G. Wen, Phys. Rev. B **65**, 165113 (2002).
[9] A. M. Polyakov, Phys. Lett. B **59** (1975) 82; Nucl. Phys. B **120** (1977) 429.
[10] X.-G. Wen, F. Wilczek and A. Zee, Phys. Rev. B **39**, 11413 (1989).
[11] L. B. Ioffe and A. I. Larkin, Phys. Rev. B **39** (1989) 8988.
[12] T. Senthil, A. Vishwanath, L. Balents, S. Sachdev and M. P. A. Fisher, Science **303** (2004) 1490.
[13] M. Hermele, T. Senthil, M. P. A. Fisher, P. A. Lee, N. Nagaosa and X.-G. Wen, Phys. Rev. B **70** (2004) 214437.
[14] A. Y. Kitaev, Ann. Phys. (N.Y.) **303**, 2 (2003).
[15] X.-G. Wen, Phys. Rev. Lett. **90**, 016803 (2003).
[16] R. Moessner and S. L. Sondhi, Phys. Rev. Lett. **86**, 1881 (2001).
[17] X.-G. Wen, Phys. Rev. Lett. **88**, 11602 (2002).
[18] X.-G. Wen, Phys. Rev. B **68**, 115413 (2003).
[19] O. I. Motrunich and T. Senthil, Phys. Rev. Lett. **89**, 277004 (2002).
[20] O. I. Motrunich and T. Senthil, Phys. Rev. B **71**, 125102 (2005).
[21] L. V. Butov, A. C. Gossard and D. S. Chemla, Nature **418**, 751 (2002).
[22] One can prove this by the method of induction. It is true for $N = 3$. Suppose it is also true for $N \leq M$. For $N = M+1$, we have $\frac{(M-1)(M-2)}{2}$ constraints which do not involve $\theta^{M+1,a}$. There are $M-1$ additional constraints which involves $\theta^{M+1,a}$. They are $\theta^{M+1,1} + \theta^{1,a} + \theta^{a,M+1} = 0$ with $a = 2, \dots, M$. ($\theta^{M+1,a} + \theta^{a,b} + \theta^{b,M+1} = 0$ with $a, b > 1$ is linear combination of above constraints and does not count.) Finally we have $\frac{M(M-1)}{2}$ constraints for $N = M+1$.
[23] S.-S. Lee and P. A. Lee, to appear in Phys. Rev. Lett. [cond-mat/0502139].
[24] The formula for change of variable in integration over Grassmann variable is $\int d\xi f(\xi) = \int \frac{d\xi}{a} f(a\xi)$.
[25] L. Susskind, Phys. Rev. D **16**, 3031 (1977).
[26] If we had allowed the π -momentum mode in the imaginary time direction we would have obtained 8-component Dirac fermion[25]. In our case, we excluded the high momentum mode in the z -direction because the massless π -mode is an artifact of the discretization of the imaginary time, $|\partial_\tau X|^2 \approx (X_{i+\tau}^* X_i + c.c.)$. In the original continuous time action the π -mode is gapped.
[27] T. W. Appelquist, M. Bowick, D. Karabali and L. C. R. Wijewardhana, Phys. Rev. D **33**, 3704 (1986).
[28] J. B. Kogut, Rev. Mod. Phys. **51**, 659 (1979).
[29] M. Levin and X.-G. Wen Phys. Rev. B **67**, 245316 (2003); *ibid.* **71**, 045110 (2005).